



## The macronutrient and micronutrient (iron and manganese) signature of icebergs

Jana Krause<sup>1</sup>, Dustin Carroll<sup>2</sup>, Juan Höfer<sup>3,4</sup>, Jeremy Donaire<sup>5,6</sup>, Eric P. Achterberg<sup>1</sup>, Emilio Alarcón<sup>4</sup>, Te Liu<sup>1</sup>, Lorenz Meire<sup>7,8</sup>, Kechen Zhu<sup>9</sup>, Mark J. Hopwood<sup>9\*</sup>

5 <sup>1</sup> GEOMAR Helmholtz Centre for Ocean Research Kiel, Kiel, Germany

<sup>2</sup> Moss Landing Marine Laboratories, San José State University, Moss Landing, California, USA

<sup>3</sup> Escuela de Ciencias del Mar, Pontificia Universidad Católica de Valparaíso, Valparaíso, Chile

<sup>4</sup> Centro FONDAP de Investigación en Dinámica de Ecosistemas Marinos de Altas Latitudes (IDEAL), Valdivia, Chile

<sup>5</sup> Facultad de Ingeniería, Universidad Andrés Bello, Viña del Mar, Chile

10 <sup>6</sup> Faculty of Sciences and Bioengineering Sciences, Vrije Universiteit Brussel, Brussels, Belgium

<sup>7</sup> Department of Estuarine and Delta Systems, Royal Netherlands Institute for Sea Research, Yerseke, The Netherlands

<sup>8</sup> Greenland Climate Research Centre, Greenland Institute of Natural Resources, Nuuk, Greenland

<sup>9</sup> Department of Ocean Science and Engineering, Southern University of Science and Technology, Shenzhen, China

*Correspondence to:* Mark J. Hopwood (Mark@sustech.edu.cn)

15 **Abstract.** Ice calved from the Antarctic and Greenland Ice Sheets or tidewater glaciers ultimately melts in the ocean contributing to sea-level rise. Icebergs have also been described as biological hotspots due to their potential roles as platforms for marine mammals and birds, and as micronutrient fertilizing agents. Icebergs may be especially important in the Southern Ocean where availability of the micronutrients iron and manganese extensively limits marine primary production. Whilst icebergs have long been described

20 as a source of iron to the ocean, their nutrient signature is poorly constrained and it is unclear if there are regional differences. Here we show that 589 ice fragments collected from floating ice in contrasting regions spanning the Antarctic Peninsula, Greenland, and smaller tidewater systems in Svalbard, Patagonia and Iceland have similar characteristic (micro)nutrient signatures with limited or no significant differences between regions. Icebergs are a minor or negligible source of macronutrients to the ocean

25 with low concentrations of NO<sub>x</sub> (NO<sub>3</sub> + NO<sub>2</sub>, median 0.51 μM), PO<sub>4</sub> (median 0.04 μM), and dissolved Si (dSi, median 0.02 μM). In contrast, icebergs deliver elevated concentrations of dissolved Fe (dFe; mean 82 nM, median 12 nM) and Mn (dMn; mean 26 nM, median 2.6 nM). A tight correlation between total dissolvable Fe and Mn ( $R^2 = 0.95$ ) and a Mn:Fe ratio of 0.024 suggested a lithogenic origin for the majority of sediment present in ice. Total dissolvable Fe and Mn retained a strong relationship with

30 sediment load (both  $R^2 = 0.43$ ,  $p < 0.001$ ), whereas weaker relationships were observed for dFe, dMn and



dSi. Sediment load for Antarctic ice (median  $9 \text{ mg L}^{-1}$ ,  $n=144$ ) was low compared to prior reported values for the Arctic. A particularly curious incidental finding was that melting samples of ice were observed to rapidly lose their sediment load, even when sediment layers were embedded within the ice and stored in the dark. Our results demonstrated that the nutrient signature of icebergs is consistent with an atmospheric  
35 source of  $\text{NO}_x$  and  $\text{PO}_4$ . Conversely, high Fe and Mn, and modest dSi concentrations, are associated with englacial sediment, which experiences limited biogeochemical processing prior to release into the ocean.

## 1 Introduction

At the interface between the cryosphere and ocean, icebergs are both physical and chemical agents via which ice-ocean interactions affect marine biogeochemical cycles (Enderlin et al., 2016; Smith Jr. et al.,  
40 2007; Helly et al., 2011). Both the calving of ice from tidewater glaciers or ice shelves, and drift of icebergs through the open ocean can induce water column mixing (Meredith et al., 2023; Helly et al., 2011). Where primary production is limited by nutrient availability, such mixing could alleviate nutrient limitation (Vernet et al., 2011). Conversely, at times of year when light limitation is critical for primary producers, increased mixing and/or iceberg cover of the ocean surface may amplify light limitation,  
45 although analyses of satellite derived chlorophyll in the Southern Ocean generally show iceberg responses ranging from no significant change to positive effects (Schwarz and Schodlok, 2009; Wu and Hou, 2017). In contrast to mixing dynamics around icebergs in the open ocean, the melting of ice in inshore regions can increase stratification of the water column, contribute to the formation of a low-salinity surface layer, affect fjord-scale circulation, and alter sea-ice dynamics (Enderlin et al., 2016; Kajanto et al., 2023; Kim  
50 et al., 2018). Both inshore and offshore iceberg dynamics are sensitive to the aspect ratios of ice, with contrasting effects from individual icebergs expected depending on the relative difference between the keel depth and the mixed layer depth. Melting ice which is confined to shallow mixed layers is more likely to enhance stratification, whereas buoyant melt released at depth could possibly drive either vertical entrainment or increased stratification. Although few surveys have characterised buoyant plumes and  
55 convection cells close to individual melting icebergs (Yankovsky and Yashayaev, 2014), existing work suggests that a large fraction of subsurface melt in both Greenland and Antarctica may remain at depth (Helly et al., 2011; Moon et al., 2018). As working close to large icebergs is challenging, melt-induced



changes in water-column structure, such as the development of buoyant plumes, are poorly constrained *in situ* and some uncertainties remain in parametrizations of the underlying melt processes (Bigg et al., 1997; Yankovsky and Yashayaev, 2014; Cenedese and Straneo, 2023). This is similarly the case in the context of approximate implementation of any resulting biogeochemical perturbations in coupled models (e.g. Laufkötter et al., 2018; Person et al., 2019). Most inferences concerning the physical effects of calved icebergs come from fjord-scale studies in regions with large calved ice fluxes around Greenland (Enderlin et al., 2016; Moon et al., 2018; Kajanto et al., 2023). Individual icebergs in colder waters, such as most of the Southern Ocean, are far more challenging to study due to their isolated nature and diluted maximum meltwater concentrations of only ~2% or less (Smith Jr. et al., 2007; Stephenson et al., 2011; Helly et al., 2011).

In addition to physical effects on the water column associated with iceberg trajectories and meltwater distribution, ice-sediment interaction may have profound biogeochemical consequences (Lin et al., 2011; Shaw et al., 2011; Barnes et al., 2018). Iceberg scouring of shallow marine sediments has direct ecological implications for marine life because shelf areas frequented by icebergs develop ecosystems functionally distinct from undisturbed environments (Gutt et al., 1996; Kim et al., 2019; Kim and Collins, 2021). Frequent iceberg disturbance from scouring also likely affects the long-term carbon sequestration potential of polar shelf sediments (Barnes et al., 2018). Whilst poorly constrained, iceberg scour could furthermore function as a component of the iceberg ‘conveyer’ via which icebergs are advection agents for terrigenous sediment into the ocean (Mugford and Dowdeswell, 2010; Dowdeswell and Dowdeswell, 1989; Hart, 1934). Icebergs have long been speculated to act as an important source of the micronutrient Fe to pelagic ecosystems via delivery of both englacial sediment and the dissolved constituents of ice melt (Raiswell et al., 2008; Hart, 1934; Lin et al., 2011). On land, glaciers and ice sheets acquire small quantities of particles and nutrients from atmospheric deposition on ice surfaces (Kjær et al., 2015; Fischer et al., 1998). More visually-pronounced sediment-rich layers are formed from basal processes whereby scouring of bedrock or overrun sediments results in layers of visibly darkened basal ice from <1 m up to ~20 m thick (Mugford and Dowdeswell, 2010; Knight et al., 2000; Anderson et al., 1980). Ice-rafted debris deposited in the ocean is thought to be primarily of englacial origin, based on the assumption that



basal ice is largely lost beneath ice shelves (Anderson et al., 1980). Yet thick sediment-rich layers are not always of basal origin. Particularly in mountainous regions, debris slump can also contribute to the formation of sediment-rich layers (Anderson et al., 1980), likely explaining ‘zebra’ stripes of sediments which can be sometimes observed embedded in ice in steep terrain around the Antarctic Peninsula.

90

The fate of both englacial and basal sediment is thought to depend strongly on the dynamics of the calving front and melt rates in the vicinity of the glacier terminus (Smith et al., 2019; Mugford and Dowdeswell, 2010). Ice tongues or shelves, which may extend kilometres beyond the grounding line with warm water circulating beneath the floating ice, as is evidenced in parts of modern-day northern Greenland (Wilson and Straneo, 2015; Schaffer et al., 2020), may experience melt rates which are certain to remove 95 practically all of the embedded basal sediment that was present at the grounding line. For example, Huhn et al., (2021) estimate a melt rate of  $8.6 \pm 1.4 \text{ m yr}^{-1}$  for the floating ice tongue of Nioghalvfjærdsbræ, NE Greenland. Conversely, under colder conditions that permit re-freezing processes, nutrient and particle-rich marine ice layers may redevelop. Formation of marine ice is observed beneath ice shelves in parts of 100 Antarctica (Joughin and Vaughan, 2004; Souchez et al., 1991) from supercooled Ice Shelf Water (Oerter et al., 1992; Souchez et al., 1991). In this case, distinct basal signatures are maintained even after the original basal ice layers which were present at the grounding line are lost. For example, particulate Fe concentrations of 13-15  $\mu\text{M}$  have been reported in marine ice formed under the Amery Ice Shelf (Herraiz-Borreguero et al., 2016). Following the calving of icebergs, peripheral, sediment-rich ice is likely to be 105 rapidly lost with icebergs depositing most ice rafted debris close to shore (Dowdeswell and Dowdeswell, 1989; Mugford and Dowdeswell, 2010). Yet the complexities of englacial sediment incorporation mean a poorly constrained fraction of iceberg-borne sediment is advected offshore and released more slowly into the water column (Anderson et al., 1980; Shaw et al., 2011). Whilst the iceberg conveyer therefore has clear implications for the delivery of (micro)nutrients associated with sedimentary sources (Lin et al., 110 2011; Raiswell, 2011; Raiswell et al., 2008), it is challenging to constrain the associated fluxes on annual timescales and especially their spatial relevance to pelagic ecosystems (Person et al., 2019).



The nutrient signature of icebergs has been commented on around Greenland, Antarctica, and in smaller catchments around Svalbard where sediment exposure of calved ice may be higher (Nomura et al., 2023; Cantoni et al., 2020; Smith Jr. et al., 2007). Icebergs are widely thought to constitute a major source of Fe, particularly particulate Fe to the ocean (Lin et al., 2011; Lin and Twining, 2012; Raiswell et al., 2016). Whilst sparsely demonstrated to date, other bioessential trace elements such as Mn, which may also extensively co-limit primary production in the Southern Ocean (Hawco et al., 2022; Latour et al., 2021; Browning et al., 2021), are expected to be delivered to the ocean by similar mechanisms (Forsch et al., 2021; Bucciarelli et al., 2001; Sedwick et al., 2000). Several studies have also hinted at considerable dissolved Si (dSi, up to 10  $\mu\text{M}$ , Meire et al., 2016) or bioaccessible nitrogen concentrations (up to 5  $\mu\text{M}$ ) within ice (Parker et al., 1978; Vernet et al., 2011). Macronutrient concentrations in glacial ice are primarily hypothesized to reflect atmospheric deposition (Vernet et al., 2011), but this signature could be substantially reworked by biogeochemical (e.g. Stibal et al., 2012) or photochemical processes (e.g. Kim et al., 2010) on ice surfaces in addition to, and potentially in combination with (Raiswell et al., 2016), the sedimentary processes described above. This may be particularly the case in regions where icebergs calve from tidewater glaciers where a higher fraction of ice is exposed to peripheral sediments and basal processes than is the case for broader ice shelves. We therefore hypothesize that the iceberg nutrient signature entering the ocean may vary regionally, although prior work suggests that variation in particulate Fe content between catchments is generally masked by the large variability within individual icebergs due to high sediment load heterogeneity (Hopwood et al., 2019, 2017).

In order to understand the significance of different physical processes which determine iceberg nutrient concentrations and the associated fluxes into the ocean, here we assess the concentration of macronutrients ( $\text{NO}_x$ , dSi and  $\text{PO}_4$ ) and micronutrients (dissolved Fe and Mn) from calved ice across multiple Arctic and Antarctic catchments. In order to investigate potential spatial and temporal biases associated with seasonal shifts and the general targeting of smaller ice fragments to collect samples, we include repeat samples from five campaigns in Nuup Kangerlua (a fjord hosting three marine-terminating glaciers in southwest Greenland) and a comparison of recently calved ice from inshore and offshore ice samples in Disko Bay (west Greenland). We hypothesize that ice calved from different regions may have



different nutrient signatures. A high Fe, high dSi signature might be expected from small tidewater systems with shallow bathymetry where ice is exposed to a high degree of sediment interaction prior to and following calving. We hypothesize that these nutrient signatures will change following iceberg calving due to the loss of sediment-rich peripheral layers from free-floating icebergs. Finally, we expect  
145 that the NO<sub>x</sub> and PO<sub>4</sub> signature of ice will be universally low and mainly reflect atmospheric deposition of these nutrients due to their limited, or negligible, net release from glacier-derived sediments on annual timescales.

## 2 Methods

Iceberg samples were collected by hand or by using nylon nets to snag ice floating fragments. Sample  
150 collection was randomized at each field site location by collecting ice samples at regular intervals along pre-defined transects. 1–5 kg ice pieces were retained in low-density polyethylene (LDPE) bags and melted at room temperature. The first 3 aliquots of meltwater were discarded to rinse the LDPE bags. Meltwater was then syringe filtered (0.2 μm, polyvinyl difluoride, Millipore) for dissolved trace metal and dissolved nutrient analysis. Some unfiltered samples were also retained for total dissolvable metal  
155 analysis. In Disko Bay (west Greenland), a targeted exercise was conducted to test whether distinct regional ice signatures could be associated with specific calving locations. During cruise GLICE (R/V Sanna, August 2022) ice collection was conducted as per other regions close to the outflow of Sermeq Kujalleq (also known as Jakobshavn Isbræ) and Eqip Sermia (west Greenland). Additionally, ice fragments were collected from two large icebergs in Disko Bay, referred to herein as fragments from  
160 Iceberg "Beluga" and Iceberg "Narwhal". These icebergs were tracked using the ship's radar by logging the coordinates and relative bearing of the approximate centre of the iceberg at regular time intervals. In Nuup Kangerlua (southwest Greenland), samples were collected on 5 repeated campaigns spanning boreal spring and summer in different years (May 2014, July 2015, August 2018, May 2019 and September 2019) to assess the reproducibility of data from the same region by different teams deploying the same  
165 methods in different months and years.



Wet sediment sub-samples were dried at 60°C to determine sediment load (dry weight of sediment per unit volume, mg L<sup>-1</sup>). Sediment load was determined for a subset of randomly collected ice samples in parallel with (micro)nutrients in the Antarctic Peninsula. In Maxwell Bay (King George Island), a targeted exercise was conducted to collect ice with embedded sediment. Eight large ice fragments (10-45 kg) with sediment layers embedded within the ice were retained in sealed opaque plastic boxes. These fragments were specifically selected to avoid the possibility of including samples with surface sediment acquired by ice scouring the coastline or shallow sediments. Boxes were half-filled with seawater from the bay. Sediment-rich ice was left to melt in the dark with an air temperature of ~5-10°C. Periodically (after 2, 4, 8, 16, 24, and 48 hours) the water was weighed and settled sediment was removed by decanting and filtration before estimating its dry weight.

For trace metal clean sample collection, LDPE sample bottles were pre-cleaned in a three-stage procedure (detergent, 1 M HNO<sub>3</sub>, and 1 M HCl) and then stored double bagged until required in the field. For macronutrient samples collected in parallel, polypropylene tubes were rinsed once with sample water. Trace metal samples were acidified to pH 1.9 by addition of 180 µL HCl (UPA, ROMIL) and allowed to stand upright for >6 months prior to analysis via inductively-coupled, plasma mass spectrometry (ICP-MS, Element XR, ThermoFisher Scientific) after dilution with 1 M HNO<sub>3</sub> (distilled in-house from SPA grade HNO<sub>3</sub>, Roth). Calibration for Fe and Mn was via standard addition with a linear peak response from 1–1000 nM (R<sup>2</sup> > 0.99). Analysis of the reference material CASS-6 yielded a Fe concentration of 26.6 ± 1.2 nM (certified 27.9 ± 2.1 nM) and a Mn concentration of 37.1 ± 0.83 nM (certified 40.4 ± 2.18 nM). A subset of samples from Equip Sermia and Nuup Kangerlua were analysed for dissolved trace metals present at lower concentrations after pre-concentration using an offline seaFAST system followed by ICP-MS exactly as per Rapp et al., (2017) with calibration for dissolved Ni, Cu via isotope dilution, and dissolved Co via standard addition. Measured values of a consensus reference material (GSP, n=8) were in relatively good agreement with consensus values (Supp. Table 1). Where macronutrient samples were not collected in parallel, samples preserved for trace metals were analysed for PO<sub>4</sub> and dSi (this was not possible for NO<sub>x</sub> because of residual contamination from concentrated HNO<sub>3</sub> in bottles). Analysis of macronutrients was conducted for NO<sub>3</sub>, NO<sub>2</sub>, PO<sub>4</sub> and dSi by segmented flow injection analysis using a



195 QUAATRO (Seal Analytical) auto-analyzer (Hansen and Koroleff, 1999). Recoveries of a certified reference solution (KANSO, Japan) were  $98 \pm 1\%$   $\text{NO}_x$ ,  $99 \pm 1\%$   $\text{PO}_4$  and  $97 \pm 3\%$  dSi. Detection limits varied between sample batches but were typically  $\sim 0.02 \mu\text{M}$   $\text{NO}_x$ ,  $0.002 \mu\text{M}$   $\text{NO}_2$ ,  $0.02 \mu\text{M}$   $\text{PO}_4$ , and  $0.04 \mu\text{M}$  dSi.

200 In addition to new data from 367 new samples collected and analysed herein, existing comparable data was compiled from prior literature and is included in the dataset to make a total of 589 samples (note that not all samples were analysed for all parameters so n varies between statistical analyses). Previously published data includes samples from Greenland, Svalbard, the Antarctic Peninsula, Patagonia and Iceland (Hopwood et al., 2019, 2017; Campbell and Yeats, 1982; De Baar et al., 1995; Höfer et al., 2019; 205 Lin et al., 2011; Loscher et al., 1997; Martin et al., 1990; Forsch et al., 2021). Throughout concentrations are reported in units  $\text{L}^{-1}$ , referring to the concentration measured in meltwater.

To test if icebergs had a distinct chemical signature depending on their origin at a hemisphere, regional and catchment scale, a multivariate PERMANOVA was realized (function `adonis2` from `vegan` package, 210 Oksanen et al., 2020) using the concentrations of trace metals (both dissolved and total dissolvable) and macronutrients ( $\text{NO}_x$ ,  $\text{PO}_4$  and dSi). Along with this analysis a non-metric MultiDimensional Scaling (nMDS, function `metaMDS` from `vegan` package, Oksanen et al., 2020) was used to compute the ordination of the iceberg samples depending on their catchment. The same analyses were used to assess differences in Disko Bay samples collected in August 2022, in this case comparing iceberg samples 215 collected in inshore and offshore zones. In both cases subsequent ANOVA (`aov` function package `stats`) and a Tuckey test (`TukeyHSD` function package `stats`) were undertaken to test for significant differences in specific trace metal and macronutrient concentrations. The relationship between iceberg sediment load and the concentration of trace metals (both dissolved and total dissolvable) and macronutrients was determined by means of a linear regression (`lm` function package `stats`). For this analysis two outliers were 220 removed from the dataset because their sediment load values were over an order of magnitude larger ( $50726 \text{ mg L}^{-1}$  and  $6128 \text{ mg L}^{-1}$ ) than other values (total  $n=144$ ); including these two data points would have disproportionately skewed the relationships. Finally, to analyse how melting and sediment release





rates changed over time using the incubations in Maxwell Bay, we used the same procedure as Höfer et al., (2018). In short, we first tested if the relationship between melting and sediment release rates and time  
225 better fitted a linear or exponential relationship using a second-order logistic regression. Then, we tested the fit of the selected relationship (exponential in this case) to see if the relationship was significant and determined the percentage of variance explained (lm function package stats). Since the initial conditions of each incubation (i.e. iceberg size, shape and initial sediment load) varied, the rates for each individual experiment were normalized by dividing each rate by the maximum rate registered in the same incubation.  
230 All statistical analyses and figures (package ggplot2) were realized using R version 4.3.2 (R Core Team, 2023).

### 3 Results

#### 3.1 Nutrient distributions and chemical signature of icebergs

Average macronutrient concentrations in ice samples were low with median concentrations of 0.04  $\mu\text{M}$   
235  $\text{PO}_4$ , 0.54  $\mu\text{M}$   $\text{NO}_3$  and 0.02  $\mu\text{M}$  dSi. A large proportion of all macronutrient samples were below detection limits and so how these samples were treated statistically made a small difference to calculated averages and relationships. Throughout the dataset  $\text{NO}_2$  was close to, or below, detection thus  $\text{NO}_3$  and  $\text{NO}_x$  concentrations were practically identical with  $\text{NO}_2$  almost invariably constituting <10% of  $\text{NO}_x$  (mean 1.8%). Mean nutrient concentrations in all cases were higher than median concentrations and the  
240 large relative standard deviations indicated that variability between samples might mask any regional differences. It has been previously reported that both total dissolvable Fe (TdFe) and dFe concentrations are extremely variable within ice samples collected at the same location (Lin et al., 2011; Hopwood et al., 2017). This remained the case with the expanded dataset herein with notable differences between the mean (82 nM dFe, 13  $\mu\text{M}$  TdFe) and median concentrations (12 nM dFe, 220 nM TdFe) on a global scale.  
245 An extremely broad range of concentrations was also observed for both dissolved Mn (mean 26 nM, median 2.6 nM) and total dissolvable Mn (TdMn; mean 150 nM, median 10 nM). As per Fe, this reflected the skewed distribution of the dataset towards a low number of samples with extremely high concentrations. The highest 2% of TdMn samples accounted for 79% of the cumulative TdMn measured.



Similarly, the highest 2% of TdFe samples accounted for 77% of the cumulative TdFe measured.  
250 Accordingly, there were very high relative standard deviations for both mean dMn ( $26 \pm 160$  nM) and  
TdMn ( $150 \pm 1500$  nM) which, as per Fe, remained high when data was grouped by region or catchment.  
Considering all (micro)nutrients measured, there were no significant differences in the iceberg chemical  
signature at a hemispheric (p value = 0.16) or regional (p value = 0.16) level. However, a PERMANOVA  
analysis showed significant differences ( $R^2 = 0.24$ , p value  $<0.001$ ) at a catchment level. Similarly, an  
255 nMDS analysis (stress = 0.07) showed that samples from the same catchment tended to be grouped closer  
together (Fig. 1) and in general Antarctic samples were distributed on the left side, whereas Arctic samples  
were more abundant on the right side of the ordination analysis (Fig. 1).

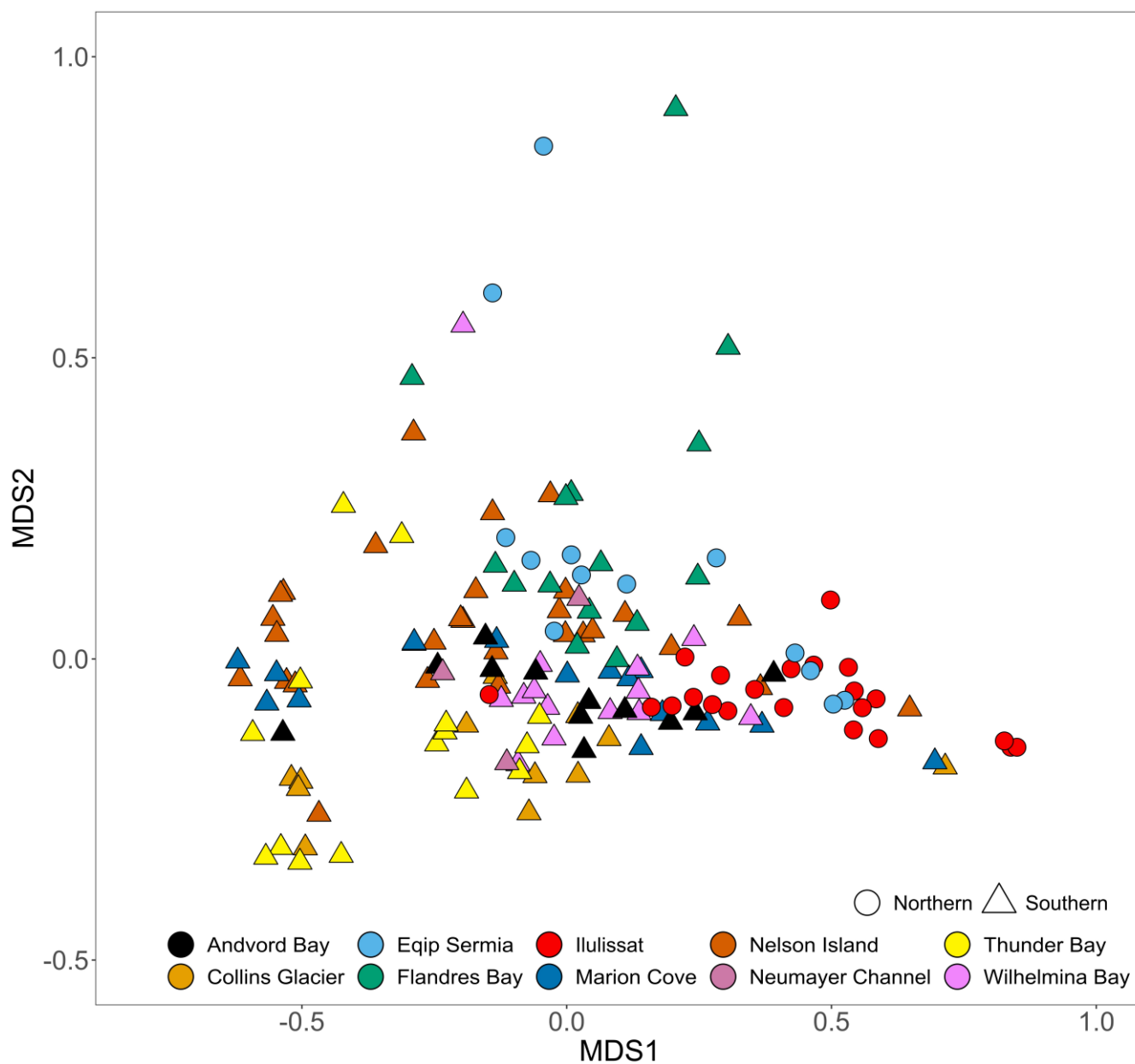


Figure 1. A scatter plot showing the results of a nMDS ordination analysis using macro- and micronutrient concentrations (only samples with complete data for the following parameters are shown: NO<sub>x</sub>, PO<sub>4</sub>, dSi, dFe, TdFe, dMn and TdMn). A PERMANOVA analysis of iceberg nutrient concentrations showed significant differences at a catchment level ( $R^2 = 0.24$ ,  $p$  value  $< 0.001$ ). Samples are grouped by hemisphere, colours denote catchments.

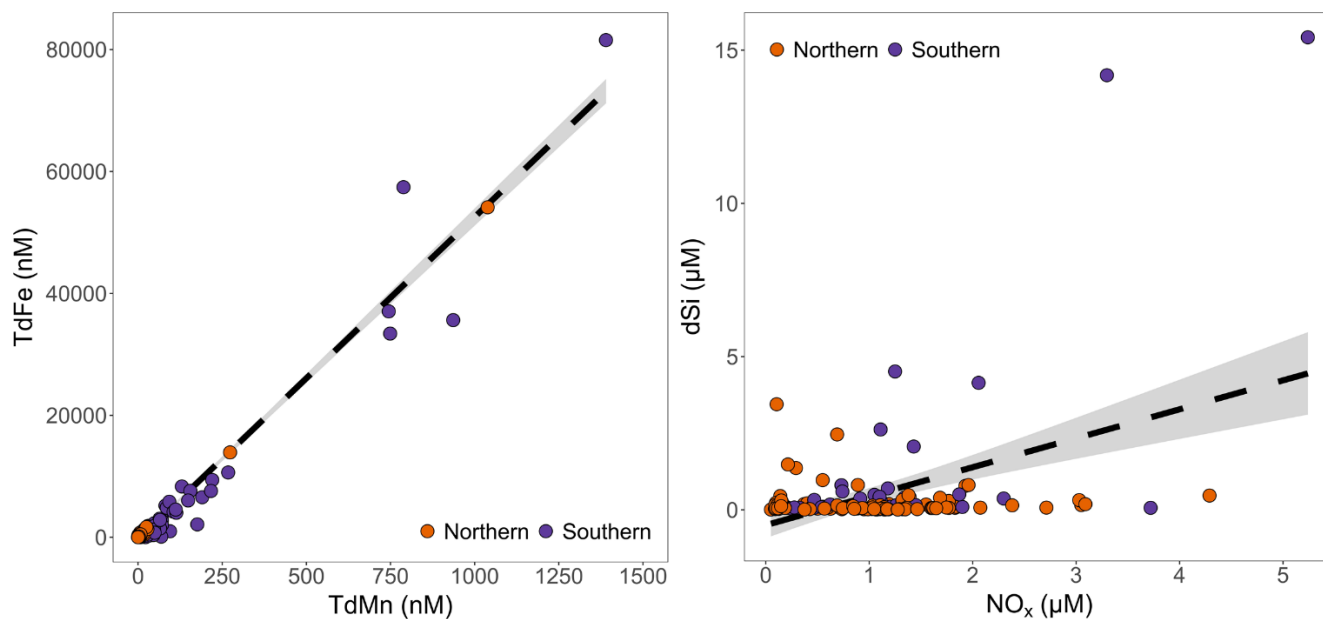


265 The ratio of TdFe:TdMn was linear ( $R^2 = 0.95$ , calculated excluding the highest 2% of Mn and Fe concentrations to avoid skewing the gradient, Fig. 2). Furthermore, the total dissolvable Mn:Fe ratio of 0.0225 (linear regression  $TdMn = 0.0225 \times [TdFe]$ ) was close to that expected from mean continental crust composition which is approximately 0.1% MnO and 5.04% FeO by weight (producing a ratio of 0.020) (Rudnick and Gao, 2004). In contrast, no clear relationship was observed between dFe and dMn.

270 For all data, all Antarctic data and all Greenlandic data, respectively, the mean dMn:dFe (0.47, 0.50 and 0.28) and median dMn:dFe (0.17, 0.19 and 0.11) ratios were consistently higher than the TdMn:TdFe ratio. This indicates an excess of dMn compared to the lithogenic ratio observed in the total dissolvable fraction. Curiously, despite the potential for dSi to be released from sedimentary phases via similar mechanisms to Fe and Mn, neither trace metal correlated well with dSi. Throughout the whole dataset,

275 dSi concentrations were low. Only 7 of 478 samples had dSi concentrations  $>10 \mu\text{M}$ , only 9.4% of samples had concentrations  $>1.0 \mu\text{M}$ , and 47% of all samples were below detection. Dissolved Si therefore had concentrations and a distribution much more like  $\text{NO}_x$  and  $\text{PO}_4$  than Mn or Fe. This was not typically the case in glacier runoff close to the sites where ice was collected (Supp. Table 2). With the exception of subglacial runoff collected on Doumer Island (South Bay, Western Antarctic Peninsula), dSi

280 concentrations in runoff were always high relative to both nitrate in runoff (typically  $\sim 12 \times [\text{NO}_x]$ ) and to the mean dSi concentration in icebergs. Doumer Island may be the exception because it consists of a small ice cap which is likely cold-based with steep topography, such that runoff-sediment interaction is limited.



285 Figure 2. A comparison of (micro)nutrient concentrations in all ice fragments where concentrations were above the detection limits. *Left* Total dissolvable Fe and total dissolvable Mn were strongly correlated ( $p$  value  $<0.001$ ,  $R^2 = 0.95$ , note the highest 2% of measured concentrations were excluded to avoid skewing the gradient. *Right* dSi and  $\text{NO}_x$  had a weak correlation ( $p$  value  $<0.001$ ,  $R^2 = 0.19$ ).

290 No significant relationship was evident between  $\text{PO}_4$  and  $\text{NO}_x$  concentrations, whereas a weak, but significant, relationship was evident between dSi and  $\text{NO}_x$  concentrations (Fig. 2). A subset of samples appeared to show a close to 1:1 relationship between dSi and  $\text{NO}_x$ , which resembles the Redfield Ratio (Redfield, 1934). A closer inspection of these points shows they accounted for about 14% of the sub-dataset where all macronutrient concentrations were detectable ( $n=22$  for those with  $[\text{NO}_x]$  and  $[\text{dSi}] >0.4$   $\mu\text{M}$ , for lower concentrations it is largely arbitrary determining whether or not samples can be assigned to the group). Samples in this group include multiple catchments but with a large component from Ilulissat (32% of datapoints) and Nuup Kangerlua (55% of datapoints), both of which were over-represented compared to their proportional importance in the sub-dataset where they each constituted 18% of datapoints. Antarctic samples and samples from Eqip Sermia were under-represented in this ~1:1 group, accounting for 0 and 2 (9%) samples, respectively, despite contributing 26% and 20% of the samples with all macronutrients detectable. The ~1:1 datapoints all refer to summertime so cannot easily be explained

295

300



as mistaken sea ice samples. Furthermore, observed nutrient concentrations were often too high to be explained by carry-over from seawater contamination (see Section 3.2). The ratios of dSi:NO<sub>3</sub> also did not consistently match the ratio in near-surface fjord water samples collected in parallel with icebergs. 305 Whilst the dSi:NO<sub>3</sub> ratio in most near-surface samples from the Ilulissat Icefjord in August 2022 was ~1 (1.39 ± 0.61, n=25 in August 2022), for Nuup Kangerlua in August and September 2019 the ratio of dSi:NO<sub>3</sub> was always >18 (Krause et al., 2021). A ~1:1 NO<sub>x</sub>:dSi ratio in ice resembles a marine origin.

### 3.2 Evaluating reproducibility and potential sampling biases

Glacial ice can usually be visually distinguished from sea ice due to its distinct texture, colour and 310 morphology. For meltwater samples that were tested for salinity, values were always <0.3 psu. However, even minor traces of seawater in samples would be sufficient to impart a measurable macronutrient signature because ice macronutrient concentrations were generally very low compared to pelagic macronutrient concentrations in the corresponding sampling regions. This is particularly the case at the Antarctic sites where high macronutrient concentrations of 20-80 µM dSi, 1-2 µM PO<sub>4</sub> and 10-30 µM 315 NO<sub>3</sub> are relatively typical of marine waters (e.g. Höfer et al., 2019; Forsch et al., 2021; Trefault et al., 2021). Close to marine-terminating glaciers in the Arctic, macronutrient concentrations in near-surface waters can still be elevated relative to the low concentrations reported for ice, e.g. 1-30 µM dSi, 0.2-0.7 µM PO<sub>4</sub> and 0-10 µM NO<sub>3</sub> for the inner part of Nuup Kangerlua (Krause et al., 2021; Meire et al., 2017). Thus, seawater macronutrient concentrations were generally equal to, or greater than ice concentrations 320 at the locations where ice calves.

Using the maximum observed marine macronutrient concentrations for our Antarctic sampling locations, assuming no detectable macronutrients in ice and that salinity of 0.3 exclusively reflected the carry-over of seawater from sampling, nutrient concentrations of up to 0.26 µM NO<sub>3</sub>, 0.02 µM PO<sub>4</sub> and 0.069 µM 325 dSi could be observed as a seawater contamination signal. The rinsing procedure used to collect samples herein whereby ice was sequentially melted, with the meltwater then used to swill and rinse the sample bag, was designed precisely to minimize trace metal contamination and three such rinses undertaken correctly would theoretically remove ~99.99% of any saline water collected with an ice sample in addition



to any contamination from ice handling. This would also not leave a detectable ( $>0.01$ ) salinity increase  
330 in the collected sample such that any detected salinity would have to come from ice melt. Sea ice samples  
were not targeted for sampling herein, but a few samples were collected during the 2017 Pia fjord  
campaign (Patagonia) and measured macronutrient concentrations were: 2.00 and 5.97  $\mu\text{M}$   $\text{NO}_x$ , 0.08 and  
0.13  $\mu\text{M}$   $\text{PO}_4$ , 0.28 and 0.63  $\mu\text{M}$  dSi. These sea ice  $\text{NO}_x$  and dSi concentrations were above average  
335 compared to freshwater ice samples collected in the same location. Similarly, samples of land fast sea ice  
from Antarctica generally have high concentrations of all macronutrients compared to iceberg samples  
reported herein (Grotti et al., 2005; Günther and Dieckmann, 1999; Nomura et al., 2023). It is apparent  
from the ratio of  $\text{NO}_x:\text{PO}_4:\text{dSi}$  in sea ice that the high nutrient signature in sea ice has a saline origin  
(Henley et al., 2023). A sequential rinsing with sea ice might lead to an uneven distribution of nutrients  
in meltwater samples due to the layered structure of sea ice and the effects of brine channels  
340 (Vancoppenolle et al., 2010; Gleitz et al., 1995; Ackley and Sullivan, 1994). With the possible exceptions  
of regions that experience ice mélange (a mixture of sea ice and icebergs) and/or marine ice, glacial ice  
is expected to be more homogenous with respect to salinity. A further critical difference with sea ice  
concerns ambient conditions during sampling as all ice samples collected herein were obtained from  
seawater with temperatures  $>0^\circ\text{C}$  i.e. under conditions where ice was melting when it was collected,  
345 whereas a large fraction of sea ice cores studied to date refer to conditions without *in situ* melt occurring.  
In prior work we also demonstrated no sustained trend in Fe concentrations when aliquots of meltwater  
were collected in series (Hopwood et al., 2016).

During the dedicated iceberg cruise campaign GLICE in Disko Bay (August 2022), ice collection was  
350 confined to 4 subregions of interest (Fig. 3, Supp. Table 3). There was partial ice cover in Disko Bay  
during boreal summer, which was mainly limited to a patch of high iceberg density close to the outflow  
of Ilulissat Icefjord. Combined with the confined nature of the coastal fjords sampled and the relatively  
fast disintegration of smaller ice fragments, it was possible to identify with a high degree of certainty the  
origin of ice within each subregion (Fig. 3). Within the fjord system hosting the marine-terminating  
355 glacier Eqip Sermia, ice fragments were highly likely to have originated from either Eqip Sermia itself  
or, if not, certainly from adjacent calving fronts in the same fjord. Similarly, close to the outflow of



Ilulissat Icefjord, ice fragments were highly likely to have originated from Sermeq Kujalleq. Ice slicks which were visibly observed to calve from two offshore icebergs within an hour prior to sample collection each constituted an additional subregion of interest. The two icebergs, referred to herein as ‘Narwhal’ and ‘Beluga’ were both isolated from other floating ice features with maximum dimensions above the waterline of >100 m width and >20 m height (Fig. 3). Radar measurements determined that ‘Narwhal’ was approximately stationary throughout the observation period (~12 hours) likely pirouetting on an area of shallow bathymetry. Iceberg ‘Beluga’ was free-floating and proceeding northwards along a trajectory through the area which hosted the highest observed iceberg densities in Disko Bay over the cruise duration (mid-August 2022).

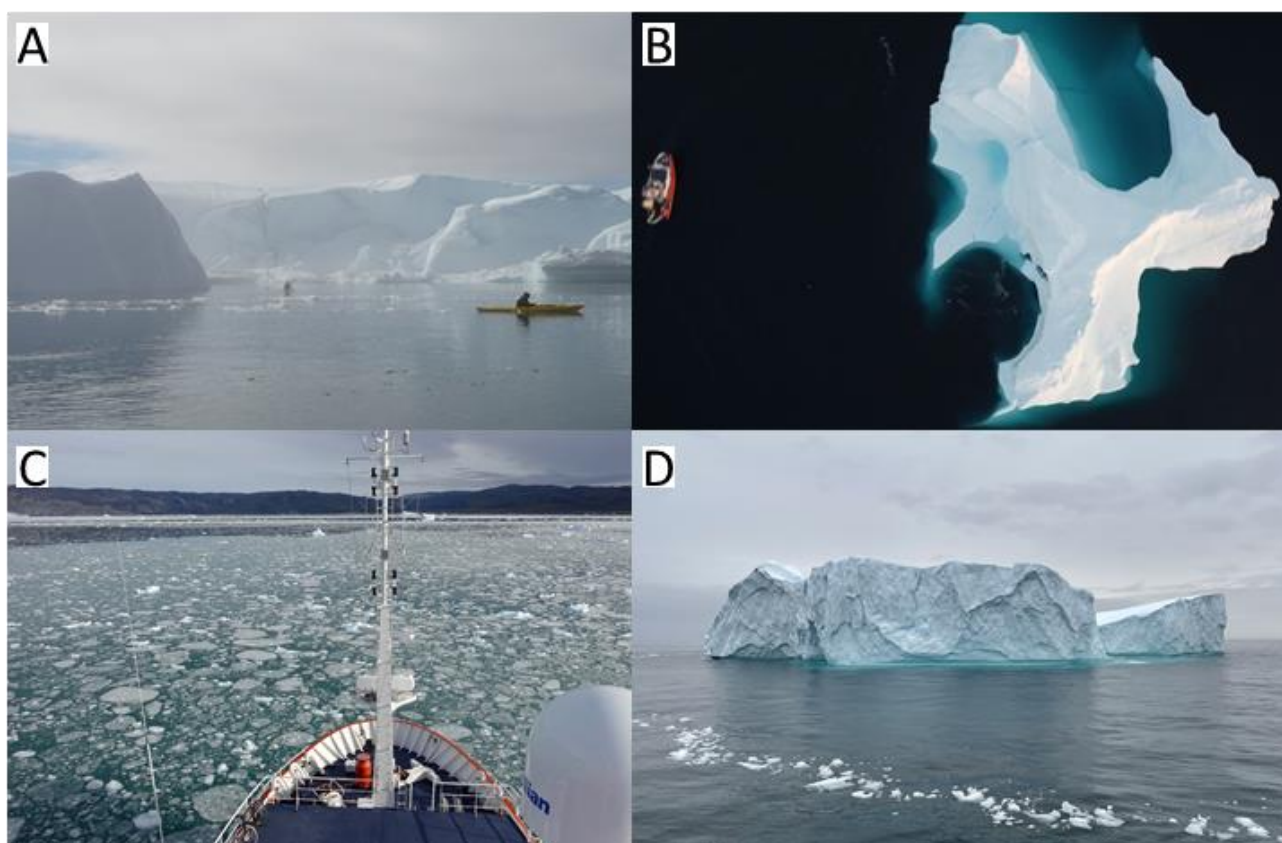


Figure 3. Ice sample collection areas in four distinct regions of Disko Bay. A Icebergs grounded on the sill at the entrance to the Ilulissat Icefjord. B An offshore iceberg which was grounded during the sampling period referred to herein as iceberg ‘Narwhal’. C Ice fragments in front of the marine-terminating glacier





370 Equip Sermia. D An offshore iceberg which was free-floating during the sampling period referred to herein as iceberg ‘Beluga’.

Ice from the 4 sampled subregions in Disko Bay was similar in all cases with overlapping ranges for the NO<sub>x</sub>, PO<sub>4</sub> and dSi concentrations of ice at different locations (Fig. 4). A PERMANOVA analysis showed  
375 small, but significant, differences ( $R^2 = 0.15$ ,  $p$  value = 0.002) in the chemical signature of iceberg samples collected inshore (Groups A and C, Fig. 3) or offshore (Groups B and D, Fig. 3) in Disko Bay when combining groups. An ordination analysis (nMDS stress = 0.04) showed that offshore icebergs were grouped together on the left side of the ordination, whereas inshore icebergs were more common on the right side of the ordination (Fig. 4). In general, offshore and inshore icebergs presented similar  
380 concentrations of all nutrients in most of the samples, except for a few inshore samples that had higher concentrations of all nutrients (Fig. 4). When testing these differences for each individual nutrient, only PO<sub>4</sub> showed significant differences between the two categories ( $p$  value = 0.035), with offshore icebergs showing lower concentrations (Fig. 4). The difference between inshore and offshore ice, whilst present, was therefore relatively modest.

385

Further insight can be gained from a comparison of all data available from Nuup Kangerlua, a relatively well-studied glacier fjord in southwest Greenland. The fjord hosts three marine-terminating glaciers with heavy ice mélangé cover observed in the inner fjord year-round and some sea ice in the inner fjord during winter. Samples were collected from the fjord during five independent field campaigns from 2014 to 2019  
390 in different seasons from May in boreal spring to September in boreal autumn. Considering the number of parameters sampled and the relatively high standard deviation of almost all parameters relative to the mean or median measured concentrations, there was limited evidence for any seasonal or inter-campaign differences (Supp. Table 4). No significant differences ( $p > 0.05$ ) were found between groups of samples obtained at the same field site when organizing the complete dataset by field site and defining each  
395 separate field campaign as a group.

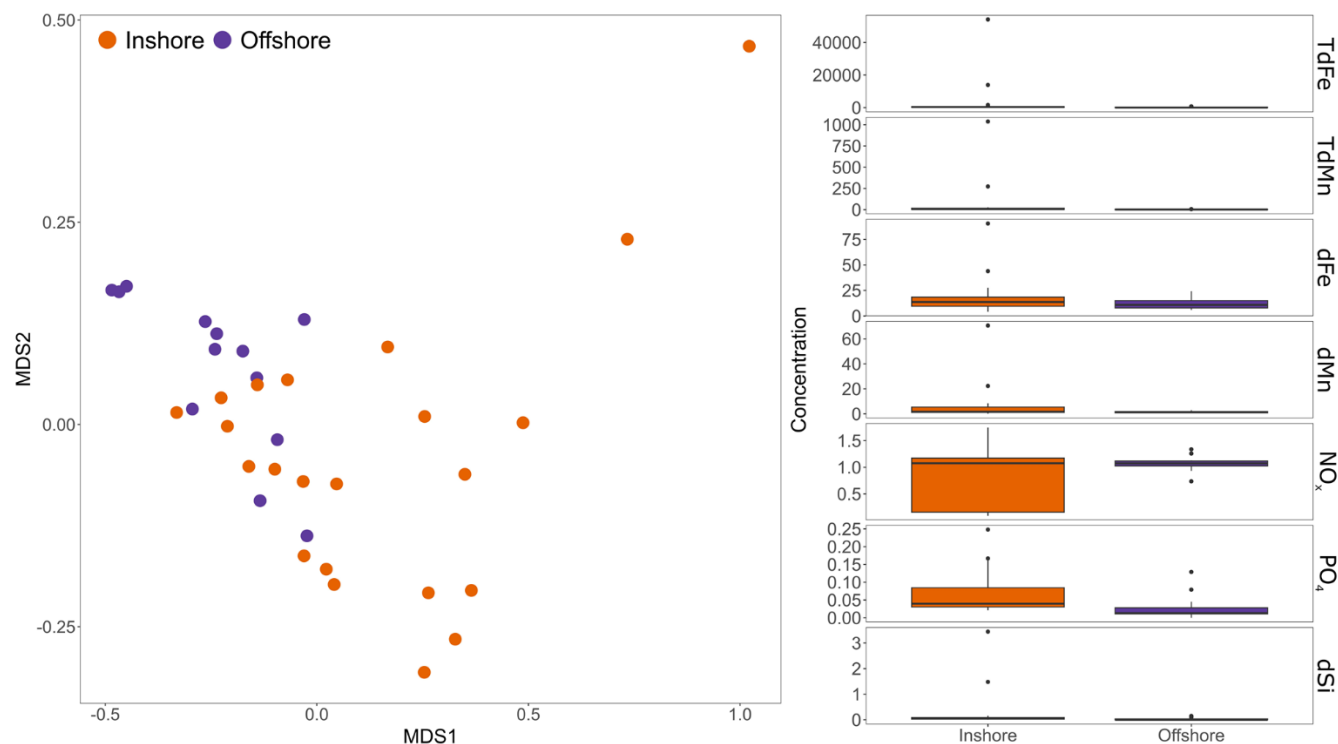


Figure 4. Comparison of nutrient concentrations from inshore and offshore ice samples collected in Disko Bay (August 2022, see Fig. 3). *Left* An ordination analysis (nMDS) comparing concentrations of all nutrients measured in ice contrasting inshore and offshore areas of Disko Bay. A PERMANOVA analysis of iceberg nutrient concentrations showed weak but significant differences between both areas ( $R^2 = 0.15$ ,  $p$  value = 0.002). *Right* A direct comparison of all nutrient concentrations for the same dataset. Units:  $\mu\text{M}$  for dSi,  $\text{NO}_x$  and  $\text{PO}_4$ ; nM for all trace metals.

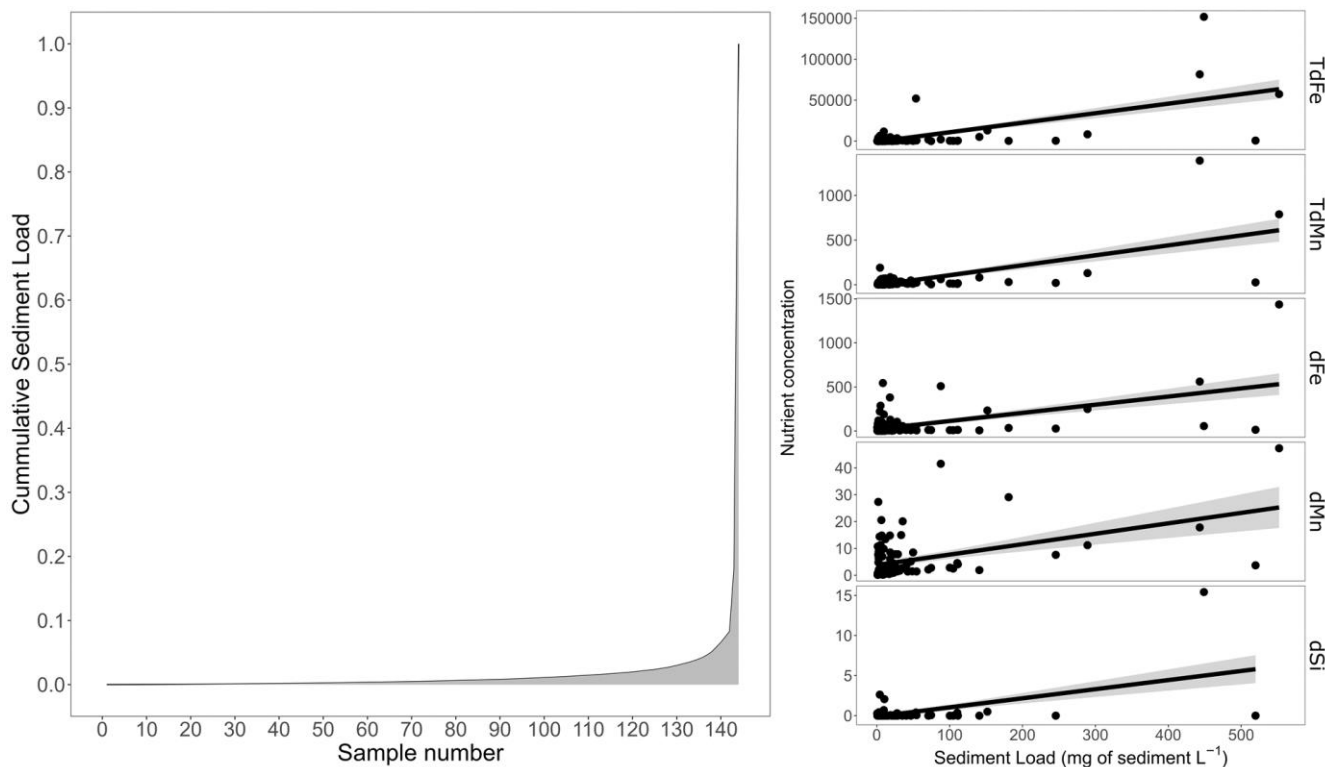
### 3.3 Sediment load within icebergs and its relationship with nutrient concentration

The sediment load within icebergs collected around the Antarctic Peninsula was highly variable with a maximum of  $5072 \text{ mg L}^{-1}$  and a minimum of  $0.69 \text{ mg L}^{-1}$  (median  $8.5 \text{ mg L}^{-1}$  and mean  $430.5 \text{ mg L}^{-1}$ ). Particle loads were assessed in three Antarctic locations. The median dry mass was similar across three areas, but the mean ( $\pm$  standard deviation) dry mass was more variable due to the occasional sample with a high sediment load. Mean dry mass across three areas was: Maxwell Bay, King George Island, (n=65)  $910 \pm 6300 \text{ mg L}^{-1}$ ; Thunder Bay and Neumayer Channel, Wiencke Island, (n=19)  $35 \pm 110 \text{ mg L}^{-1}$ ; and



410 South Bay, Doumer Island, (n=60)  $39 \pm 98 \text{ mg L}^{-1}$ . Median sediment loads in the three regions were 12, 2.5 and  $7.7 \text{ mg L}^{-1}$ , respectively. The heterogeneous distribution of sediments was reflected in the fact that ~2% of samples collected contributed ~90% of the total sediment retrieved from the iceberg samples collectively (Fig. 5). This distribution is similar to previous analysis regarding TdFe (Hopwood et al., 2019), and sediment load in icebergs from Svalbard (Hopwood et al., 2017). It also qualitatively matches  
415 the distribution of TdMn and TdFe observed herein (see Section 3.1).

As Fe, Mn and dSi may have sedimentary origins, we tested if there were any significant relationships between the sediment load of an iceberg and the concentration of each macronutrient and both total dissolvable and dissolved trace metals (Fig. 5). For  $\text{NO}_x$  and  $\text{PO}_4$  there was no significant relationship  
420 between sediment load and concentration (p values of 0.18 and 0.26 respectively). This is consistent with the hypothesis that these nutrients primarily have an atmospheric deposition origin which contributes only a minor fraction of the sediment load to bulk ice. Conversely, TdFe, TdMn, dFe, dMn and dSi all had significant relationships with sediment load. The concentrations of the total dissolvable fraction of trace metals showed better fits (TdFe  $R^2 = 0.43$ , p value  $<0.001$ ; TdMn  $R^2 = 0.43$ , p value  $<0.001$ ), than the  
425 dissolved phases of metals (dFe  $R^2 = 0.30$ , p value  $<0.001$ ; dMn  $R^2 = 0.20$ , p value  $<0.001$ ) and dSi ( $R^2 = 0.28$ , p value  $<0.001$ ). This is consistent with the expectation that englacial sediment drives a direct enrichment in TdFe and TdMn, which increase proportionately with sediment load, whereas the enrichment of dFe, dMn and dSi is more variable and depends on the specific conditions that sediment and ice experience between englacial sediment incorporation and sample collection.



430

435

Figure 5. Iceberg sediment load and its relationship with nutrient concentrations. *Left* The uneven distribution of sediment in randomly collected ice samples from the Antarctic Peninsula. *Right* The relationship between nutrient concentrations and sediment load for ice samples from the Antarctic Peninsula. Only significant ( $p$  value  $<0.001$ ) relationships are shown. No significant relationship was evident for sediment load with nitrate or phosphate. Units:  $\mu\text{M}$  for dSi, nM for all trace metals.

440

On several occasions in Nuup Kangerlua and Maxwell Bay we observed structures up to several centimetres wide/deep on iceberg surfaces akin to cryoconite holes both above and below the waterline. The sediment within such holes was easily disturbed when approaching ice fragments. The regular agitation and movement of floating ice fragments and the chaotic nature of calving events suggests that cryoconite holes on icebergs formed *in situ* rather than being relics of a glacier surface prior to calving. This raises an interesting question about whether sediment-rich layers and any associated nutrients could be subject to disintegration mechanisms distinct from bulk ice. When large ice samples weighing 10-45 kg were stored in the dark at 5-10°C, higher loads of sediment were released in the initial melt fractions



445 (Supp. Fig. 1). This trend was highly reproducible occurring in all observed experiments (n=8) when large ice samples specifically targeted for their high englacial sediment loads were retained. The sediment release rate declined with a logarithmic function over the first 48 hours (Supp. Figure 1). It should be noted that randomly collected samples had much lower sediment loads (Fig. 5).

### 3.4 Concentrations of dissolved Co, Ni and Cu

450 The high concentrations of Fe and Mn present in some samples created some analytical challenges in attempting to pre-concentrate samples to quantify lower abundance elements. After analysis of all samples via dilution for Fe and Mn, two complete batches of samples, each representing all of the ice collected during one field campaign (from Eqip glacier and from Nuup Kangerlua), were selected for trace metal analysis via pre-concentration. Both batches were representative of the larger dataset for macronutrients,  
455 Fe and Mn, yet neither contained samples within the highest 2% of measured Fe concentrations. Mean ( $\pm$  standard deviation) dissolved trace metal samples were  $21 \pm 22$  pM dissolved Co,  $0.36 \pm 0.45$  nM dissolved Ni, and  $0.39 \pm 0.40$  nM dissolved Cu (Supp. Table 5). There was a strong correlation between most combinations of elements which suggests a common origin for dissolved trace elements. Dissolved concentrations of Co, Ni and Cu were all relatively low compared to concentrations expected in other  
460 freshwater environments (Supp. Table 5). Mean concentration were low compared to both the freshwater endmembers derived for the Arctic and northeast Greenland shelf in prior work (Charette et al., 2020; Krisch et al., 2022), and concentrations measured in runoff at sites in west Greenland and the Western Antarctic Peninsula (Krause et al., 2021; Hawkings et al., 2020).

## 4 Discussion

### 465 4.1 Insights into nutrient origins from ratios

There are several distinct mechanisms via which ice could accumulate different nutrient signatures. Precipitation and aerosol deposition on ice surfaces would be expected to impart an atmospheric deposition signature (Kjær et al., 2015; Fischer et al., 1998), assuming a limited biogeochemical imprint from surface biological (or photochemical) processes. Atmospheric deposition of  $\text{NO}_x$  and  $\text{PO}_4$  varies  
470 regionally. Snow  $\text{NO}_3$  deposition over central Greenland is reported as  $1.21 \pm 0.19$   $\mu\text{mol kg}^{-1}$  for recent



and  $0.56 \pm 0.19 \mu\text{mol kg}^{-1}$  for pre-industrial values (Fischer et al., 1998). Concentrations of  $\text{PO}_4$  are more sensitive to the method used due to universally low concentrations. Phosphate concentrations in ice from the last glacial period in Greenland are reported to range from 3 to 62 nM (Kjær et al., 2015). These ranges are similar to the  $\text{NO}_3$  and  $\text{PO}_4$  values we report for Greenlandic calved ice herein: mean ( $\pm$  standard deviation)  $0.78 \pm 0.69 \text{ NO}_3$ , median  $0.74 \text{ NO}_3$ , mean  $36 \pm 50 \text{ nM PO}_4$ , and median  $28 \text{ nM PO}_4$ . Modern atmospheric deposition is expected to impact the N:P ratio as atmospheric pollution is generally associated with higher N:P ratios (e.g. Peñuelas et al., 2012) and could explain the increase in N:P ratio at higher  $\text{NO}_3$  concentrations.

480 In addition to an atmospheric deposition signal in ice macronutrient concentrations, some degree of sedimentary signal is also expected to affect dSi concentrations, but not  $\text{NO}_3$  or  $\text{PO}_4$ , which is verified by the correlations herein (Fig. 5). Sediment associated with an iceberg could be from basal layers, other englacial sediment entrained prior to calving, or acquired from scouring events subsequent to calving. Shallow areas of all field sites herein had grounded icebergs. In Disko Bay during 2 weeks of cruise observations in August 2022, the majority of large ( $>100 \text{ m}$  width above water line) icebergs were 485 observed to be grounded. In terms of TdFe, TdMn, dFe, dMn and dSi we hypothesize that two categories of sediment may be distinguishable. Englacial sediment with little biogeochemical processing should retain a TdFe:TdMn ratio which is close to the crustal abundance ratio of Fe:Mn, with low dFe, dMn and dSi concentrations. Basal sediment layers, particularly from catchments with warm-based glaciers, may 490 have a similar TdFe:TdMn ratio but higher concentrations of dFe, dMn and dSi due to more active biogeochemical processing in subglacial environments (e.g. Wadham et al., 2010; Tranter et al., 2005). Finally, scoured sediments acquired after calving could constitute a broad range of compositions considering the gradient in benthic conditions along glacier fjords (Laufer-Meiser et al., 2021; Wehrmann et al., 2013) and may accordingly contain more biogenic and/or authigenic phases than englacial sediment. 495 These sediments may be highly variable in composition but should impart high TdFe and TdMn concentrations, with varying Fe:Mn ratios, and high dFe, dMn and dSi concentrations. Basal sediments and scoured sediments from fjord environments therefore probably cannot be distinguished unambiguously from concentrations measured herein alone, but we can likely distinguish englacial



500 sediment from basal or scoured sediment. Dissolved Si concentrations were low across the whole dataset, suggesting basal ice was a very small component of sampled ice. The linear relationship between TdFe and TdMn across a wide range of observed concentrations also suggests minimal incorporation of authigenic mineral phases and, in combination with low dSi, hints that basal ice from warm-based glaciers is largely absent from this dataset. This is consistent with the hypothesis that basal layers are lost prior to, or rapidly following, iceberg calving.

505

In runoff sampled close to iceberg sampling regions, only dSi concentrations tended to be elevated (Supp. Table 2). The weak, but significant relationships, with dSi, dFe, dMn and sediment load; and the stronger relationships between TdFe and TdMn and sediment load is consistent both with a sedimentary origin of these components and the caveats that further physical and/or biogeochemical processing mechanisms have to be considered to fully explain the distributions of dSi, dFe and dMn (Fig. 5). As the concentrations of NO<sub>x</sub> and PO<sub>4</sub> were consistent with an atmospheric origin, a varying concentration of dSi from sedimentary sources could also easily explain the observed trend in the N:Si and P:Si ratios. Whilst elevated dFe and dMn concentrations reflect release of these phases from glacier-derived sediments (Hawkings et al., 2020), the concentrations were not strongly correlated with each other or sediment load (Fig. 5). This could reflect the origin of dissolved metals from different mineral phases, yet dFe generally correlates poorly with other trace elements in aquatic environments due to rapid scavenging onto particle surfaces and aggregation of colloids (which are included within the '<0.2 μm' definition of dissolved herein) (Zhang et al., 2015). A poor correlation could also therefore reflect the tendency for dissolved Fe species to become scavenged. Measured concentrations refer to freshly collected meltwater so it is difficult to establish how dFe concentrations may have changed during the ice melting process. Conversely, dissolved Mn species are more stable in solution and this is often reflected in much higher dMn:dFe ratios in proglacial aquatic environments than would be expected based on crustal abundances (Hawkings et al., 2020; van Genuchten et al., 2022; Yang et al., 2022). Curiously, dSi also correlated poorly with all metal phases. This again could simply reflect different mineral phases driving elevated dSi, dFe and dMn concentrations (van Genuchten et al., 2022). Yet considering all of these elements are expected to be released from sediments, at least within specific regions some degree of correlation might

510

515

520

525



be expected. Further work to quantify the rates of gross and net dFe, dMn and dSi release under *in situ* conditions within ice and frozen sediment layers, could perhaps elucidate processes via which net release of these components may be uncoupled. Photochemical processes are likely to affect particularly Fe and Mn release (Kim et al., 2010), and the scavenging potential of Mn and Fe species (van Genuchten et al., 2022) may be important in terms of how they interact with other dissolved and particulate components of the ice-sediment matrix.

#### 4.2 Key role of sediment-rich layers, and their disintegration, for nutrient release

Several works have speculated that Arctic and Antarctic icebergs may have distinct differences in sediment load, with the former generally having higher sediment loads than the later (Anderson et al., 1980). However, there are several observer biases in making such comparisons. Arctic icebergs are generally smaller due to the prevalence of tidewater glacier-derived ice rather than large ice shelves, and Arctic icebergs are more easily observed in coastal environments than Antarctic icebergs. Ice observed at a distance often appears cleaner than is the case upon closer inspection where sediment layers can be better identified. Nevertheless, a comparison of smaller ice fragments from Kongsfjorden in Svalbard and three localities in the Antarctic Peninsula showed that the former had higher sediment loads. Mean sediment loads of 21 g L<sup>-1</sup> (median 0.58 g L<sup>-1</sup>) were previously reported for Kongsfjorden (Hopwood et al., 2019). Mean and median sediment load for ice fragments handled similarly from Maxwell Bay, Thunder Bay and South Bay were 75 mg L<sup>-1</sup> and 3.8 mg L<sup>-1</sup>, respectively, which are considerably lower. Contrasting warm/cold-based glaciers and the higher exposed land/ice cover ratio of the coastal glaciated Arctic may explain much of this difference.

Sediment-rich layers within icebergs have long been hypothesized to be particularly important for the delivery of the micronutrient Fe into the ocean (Hart, 1934) and this has been explicitly confirmed with measurements of dFe and particulate Fe (Lin et al., 2011; Raiswell, 2011). We verify herein, that sediment distribution is a major factor explaining TdFe and TdMn distribution, and a minor factor in explaining dFe, dMn and dSi distribution in icebergs (Fig. 5). The dynamics of sediment-rich layers and their fate in the marine environment is therefore of special interest for trace metal biogeochemistry given the (co)-





555 limiting role these micronutrients have for phytoplankton growth in the Southern Ocean (Martin et al., 1990; Hawco et al., 2022). The close association of TdFe and TdMn is perhaps unsurprising and corroborates a lithogenic origin for the vast majority of Fe present in icebergs. It also suggests limited biogeochemical processing of englacial material and/or rapid loss of basal ice layers preventing the modification of a lithogenic signature (Forsch et al., 2021).

560

A curious observation herein was that cryoconite formation was observed on ice fragments suggesting that, as is the case on glacier surfaces (Rozwalak et al., 2022; Cook et al., 2015), this can be an important process affecting sediment dynamics on icebergs. The unstable nature of icebergs means that cryoconite holes are likely to be shorter lived than their glacier counterparts, but they still may constitute an important feature via which iceberg embedded sediment is processed. The accumulation of sediment as cryoconite could for example impede photochemical processing of particles, but also potentially create micro-gradients in O<sub>2</sub>, pH and temperature that result in different chemical conditions than if particles were homogenously distributed (Rozwalak et al., 2022). On larger, more stable icebergs, cryoconite may facilitate the growth of attached diatoms (Ferrario et al., 2012; Robison et al., 2011). These processes are well described on ice surfaces but a critical difference in interpreting their significance in iceberg environments is that iceberg movement and rolling is likely to prevent the long-term development of cryoconite on anything other than large tabular icebergs. Nevertheless, the observation of such holes at centimetre size in environments where icebergs are free floating and rapidly disintegrating suggests that they might constitute an underappreciated mechanism of iceberg melt and sediment processing.

575

A further, to our knowledge, novel observation was the tendency of embedded sediment to be rapidly discharged from ice fragments. When collecting larger ice pieces it was found that, in all cases, embedded sediment was rapidly washed out of the ice fragments largely within the melting of the first 10-20% of ice volume (Supp. Fig. 1). These ice fragments were specifically targeted to avoid ice with surface sediment layers and so this result cannot be explained by the loss of sediment frozen on the surface of ice. If this process was occurring at larger scales in nature it could further act to skew the deposition of iceberg-borne particles towards inshore environments i.e. it would compound the inefficiencies in the delivery of

580



sediment and associated nutrients to the offshore marine environment due to the rapid loss of basal ice layers. The mechanism of this process is unclear but it is not associated with ongoing cryoconite formation or similar associated processes due to albedo effects because the ice was stored in the dark. We therefore  
585 hypothesize that sediment-rich layers in calved icebergs may be structurally weaker and thus more prone to rapid disintegration than bulk low-sediment ice.

## 5 Conclusions

A key finding throughout was that the macronutrient and micronutrient content of ice was relatively  
590 similar between catchments and regions worldwide despite the contrasting geographic context of Arctic and Antarctic ice calving fronts and notable differences in sediment loads between regions (Fig. 1). There was limited evidence of differences in ice nutrient signatures between field campaigns returning to the same location (Nuup Kangerlua, southwest Greenland) in different seasons/years and similarly limited evidence of differences contrasting ice fragments collected offshore in Disko Bay (west Greenland) with  
595 ice fragments collected inshore close to marine-terminating glacier fronts (Fig. 4). Local processes within individual catchments, rather than regional changes in climate and geology, appear to be the major driver of variability in iceberg nutrient load. On a global scale, the macronutrient content of ice is consistent with an atmospheric origin of  $\text{NO}_x$  and  $\text{PO}_4$  supplemented with small amounts of dSi from sedimentary sources.

600

Due to high heterogeneity in (micro)nutrient concentrations, especially for Fe and Mn, further sample collection would therefore not likely reduce uncertainties in fluxes associated with iceberg melt although some specific issues could be addressed. Herein we have considered only  $\text{NO}_x$  as a source of bioaccessible nitrogen, but considering the universally low concentrations, other N sources (e.g. DON- Dissolved  
605 Organic Nitrogen, and  $\text{NH}_4$ ) may be relatively important. We hypothesized that a basal ice signature would be present in some ice fragments with high dSi alongside dFe and dMn, but conversely found very low dSi concentrations across all field locations. Future process studies might elucidate the mechanistic reasons why elevated dSi concentrations are not present alongside dFe and dMn concentrations in ice melt. Finally, sediment rich layers of large ice samples were observed to rapidly melt, potentially



610 indicating that these layers are prone to disintegration. Such a mechanism could be an important regulator of sediment dispersion in the marine environment, potentially further skewing the delivery of iceberg rafted debris and nutrients towards coastal waters.

Nutrient	Greenland Ice Sheet annual discharge	Antarctic Ice Sheet annual discharge
	Mmol yr <sup>-1</sup>	Mmol yr <sup>-1</sup>
NO <sub>3</sub>	389 ± 345 (370)	418 ± 796 (168)
PO <sub>4</sub>	18 ± 25 (14)	76 ± 83 (58)
dSi	212 ± 701 (27)	476 ± 2187 (b/d)
dFe	7.1 ± 15 (3.9)	130 ± 472 (18)
dMn	2.3 ± 6.0 (0.77)	32 ± 191 (3.3)

615 Table 1. Annual fluxes of nutrients associated with icebergs assuming calved ice volume of 500 km<sup>3</sup> yr<sup>-1</sup> from Greenland and 1100 km<sup>3</sup> yr<sup>-1</sup> from Antarctica (Bamber et al., 2018; Rignot et al., 2013). Values are mean ± standard deviation (median). ‘b/d’ represents a median sample below detection.

In summary, iceberg-derived macronutrient fluxes are likely minor in terms of annual polar pelagic nutrient cycling (Table 1) and in most coastal environments will dilute, rather than enhance, 620 concentrations of NO<sub>x</sub>, PO<sub>4</sub> and dSi; especially in Antarctic waters where macronutrient concentrations are very high. Delivery of both particulate and dissolved Fe and Mn concentrations are however considerable and may act to supply marine ecosystems with sources of these micronutrients depending on the seasonal and spatial distribution of iceberg melt.

## 6 Data availability

625 New data presented herein is available from SeaDataNet [under review 6-13-2023]. Literature data was compiled from prior published values (Hopwood et al., 2019, 2017; Campbell and Yeats, 1982; De Baar et al., 1995; Höfer et al., 2019; Lin et al., 2011; Loscher et al., 1997; Martin et al., 1990; Forsch et al., 2021). For convenience, a merged dataset is appended.



## 7 Author contribution

630 MH, DC, JH and EPA designed the study and acquired funding and resources. JK, DC, JD, IH, EA, TL, LM and MH conducted field work. EA, KZ and MH conducted laboratory analysis. JK, JH and MH conducted data analysis. JK and MH wrote the initial draft of the paper and all authors contributed to revision of the text.

## 8 Competing interests

635 The authors declare that they have no conflict of interest.

## 9 Acknowledgements

Tim Steffens (GEOMAR) is thanked for technical assistance with ICP-MS, André Mutzberg (GEOMAR) for macronutrient data, Stephan Krisch (formerly GEOMAR), Thomas Juul-Pedersen (GINR) and Case van Genuchten (GEUS) for assistance with sampling. The captain and crew of RV Sanna are thanked for  
640 field support. Antarctic sampling was possible through FONDAP-IDEAL 15150003 and FONDECYT-Regular 1211338 (awarded to JH). MH received support from the DFG (HO 6321/1-1), the GLACE project organised by the Swiss Polar Institute and supported by the Swiss Polar Foundation, NSFC project 42150610482 and the European Union H2020 research and innovation programme under grant agreement n° 824077. LM was funded by research programme VENI with project number 016.Veni.192.150  
645 financed by the Dutch Research Council (NWO). JD was sponsored by a scholarship from the Instituto Antártico Chileno (INACH), Correos de Chile, and the Fuerza Aérea de Chile (FACH). Ship time and work in Nuup Kangerlua was conducted in collaboration with MarineBasis-Nuuk, part of the Greenland Ecosystem Monitoring project (GEM). We gratefully acknowledge logistics and funding contributions from the Danish Centre for Marine Research (DCH), Greenland Institute of Natural Resources, Novo  
650 Nordic Foundation (NNF17SH0028142) and INACH.



## 10 References

- Ackley, S. F. and Sullivan, C. W.: Physical controls on the development and characteristics of Antarctic sea ice biological communities— a review and synthesis, *Deep Sea Research Part I: Oceanographic Research Papers*, 41, 1583–1604, [https://doi.org/10.1016/0967-0637\(94\)90062-0](https://doi.org/10.1016/0967-0637(94)90062-0), 1994.
- 655 Anderson, J. B., Domack, E. W., and Kurtz, D. D.: Observations of Sediment-laden Icebergs in Antarctic Waters: Implications to Glacial Erosion and Transport, *Journal of Glaciology*, 25, 387–396, <https://doi.org/10.3189/S0022143000015240>, 1980.
- De Baar, H. J. W., De Jong, J. T. M., Bakker, D. C. E., Loscher, B. M., Veth, C., Bathmann, U., and Smetacek, V.: Importance of iron for plankton blooms and carbon dioxide drawdown in the Southern Ocean, *Nature*, 373, 412–415, <https://doi.org/10.1038/373412a0>, 1995.
- 660 Bamber, J. L., Tedstone, A. J., King, M. D., Howat, I. M., Enderlin, E. M., van den Broeke, M. R., and Noel, B.: Land Ice Freshwater Budget of the Arctic and North Atlantic Oceans: 1. Data, Methods, and Results, *J Geophys Res Oceans*, 123, 1827–1837, <https://doi.org/10.1002/2017JC013605>, 2018.
- Barnes, D. K. A., Fleming, A., Sands, C. J., Quartino, M. L., and Deregibus, D.: Icebergs, sea ice, blue carbon and Antarctic climate feedbacks, *Philosophical Transactions of the Royal Society A: Mathematical, Physical and Engineering Sciences*, 376, 20170176, <https://doi.org/10.1098/rsta.2017.0176>, 2018.
- 665 Bigg, G. R., Wadley, M. R., Stevens, D. P., and Johnson, J. A.: Modelling the dynamics and thermodynamics of icebergs, *Cold Reg Sci Technol*, 26, 113–135, [https://doi.org/10.1016/S0165-232X\(97\)00012-8](https://doi.org/10.1016/S0165-232X(97)00012-8), 1997.
- Browning, T. J., Achterberg, E. P., Engel, A., and Mawji, E.: Manganese co-limitation of phytoplankton growth and major nutrient drawdown in the Southern Ocean, *Nat Commun*, 12, 884, <https://doi.org/10.1038/s41467-021-21122-6>, 2021.
- 670 Bucciarelli, E., Blain, S., and Treguer, P.: Iron and manganese in the wake of the Kerguelen Islands (Southern Ocean), *Mar Chem*, 73, 21–36, [https://doi.org/10.1016/S0304-4203\(00\)00070-0](https://doi.org/10.1016/S0304-4203(00)00070-0), 2001.
- Campbell, J. A. and Yeats, P. A.: The distribution of manganese, iron, nickel, copper and cadmium in the waters of Baffin Bay and the Canadian Arctic Archipelago, *Oceanologica Acta*, 5, <https://doi.org/10.1007/s00128-002-0077-7>, 1982.
- Cantoni, C., Hopwood, M. J., Clarke, J. S., Chiggiato, J., Achterberg, E. P., and Cozzi, S.: Glacial drivers of marine biogeochemistry indicate a future shift to more corrosive conditions in an Arctic fjord, *J Geophys Res Biogeosci*, 125, e2020JG005633, <https://doi.org/10.1029/2020JG005633>, 2020.
- 675 Cenedese, C. and Straneo, F.: Icebergs Melting, *Annu Rev Fluid Mech*, 55, 377–402, <https://doi.org/10.1146/annurev-fluid-032522-100734>, 2023.
- Charette, M. A., Kipp, L. E., Jensen, L. T., Dabrowski, J. S., Whitmore, L. M., Fitzsimmons, J. N., Williford, T., Ulfso, A., Jones, E., Bundy, R. M., Vivancos, S. M., Pahnke, K., John, S. G., Xiang, Y., Hatta, M., Petrova, M. V, Heimbürger-Boavida, L.-E., Bauch, D., Newton, R., Pasqualini, A., Agather, A. M., Amon, R. M. W., Anderson, R. F., Andersson, P. S., Benner, R., Bowman, K. L., Edwards, R. L., Gdaniec, S., Gerringa, L. J. A., González, A. G., Granskog, M., Haley, B., Hammerschmidt, C. R., Hansell, D. A., Henderson, P. B., Kadko, D. C., Kaiser, K., Laan, P., Lam, P. J., Lamborg, C. H.,



- Levier, M., Li, X., Margolin, A. R., Measures, C., Middag, R., Millero, F. J., Moore, W. S., Paffrath, R., Planquette, H., Rabe, B., Reader, H., Rember, R., Rijkenberg, M. J. A., Roy-Barman, M., Rutgers van der Loeff, M., Saito, M., Schauer, U., Schlosser, P., Sherrell, R. M., Shiller, A. M., Slagter, H., Sonke, J. E., Stedmon, C., Woosley, R. J., Valk, O., van Ooijen, J., and Zhang, R.: The Transpolar Drift as a Source of Riverine and Shelf-Derived Trace Elements to the Central Arctic Ocean, *J Geophys Res Oceans*, 125, e2019JC015920, <https://doi.org/10.1029/2019JC015920>, 2020.
- Cook, J., Edwards, A., Takeuchi, N., and Irvine-Fynn, T.: Cryoconite: The dark biological secret of the cryosphere, *Progress in Physical Geography: Earth and Environment*, 40, 66–111, <https://doi.org/10.1177/0309133315616574>, 2015.
- Dowdeswell, J. A. and Dowdeswell, E. K.: Debris in Icebergs and Rates of Glaci-Marine Sedimentation: Observations from Spitsbergen and a Simple Model, *J Geol*, 97, 221–231, <https://doi.org/10.1086/629296>, 1989.
- Enderlin, E. M., Hamilton, G. S., Straneo, F., and Sutherland, D. A.: Iceberg meltwater fluxes dominate the freshwater budget in Greenland’s iceberg-congested glacial fjords, *Geophys Res Lett*, 43, <https://doi.org/10.1002/2016GL070718>, 2016.
- Ferrario, M. E., Cefarelli, A. O., Robison, B., and Vernet, M.: *Thalassioneis signyensis* (bacillariophyceae) from northwest Weddell Sea icebergs, an emendation of the generic description, *J Phycol*, 48, 222–230, <https://doi.org/10.1111/j.1529-8817.2011.01097.x>, 2012.
- Fischer, H., Wagenbach, D., and Kipfstuhl, J.: Sulfate and nitrate firm concentrations on the Greenland ice sheet: 1. Large-scale geographical deposition changes, *Journal of Geophysical Research: Atmospheres*, 103, 21927–21934, <https://doi.org/10.1029/98JD01885>, 1998.
- Forsch, K. O., Hahn-Woernle, L., Sherrell, R. M., Rocanova, V. J., Bu, K., Burdige, D., Vernet, M., and Barbeau, K. A.: Seasonal dispersal of fjord meltwaters as an important source of iron and manganese to coastal Antarctic phytoplankton, *Biogeosciences*, 18, 6349–6375, <https://doi.org/10.5194/bg-18-6349-2021>, 2021.
- van Genuchten, C. M., Hopwood, M. J., Liu, T., Krause, J., Achterberg, E. P., Rosing, M. T., and Meire, L.: Solid-phase Mn speciation in suspended particles along meltwater-influenced fjords of West Greenland, *Geochim Cosmochim Acta*, 326, 180–198, <https://doi.org/10.1016/j.gca.2022.04.003>, 2022.
- Gleitz, M., v.d. Loeff, M. R., Thomas, D. N., Dieckmann, G. S., and Millero, F. J.: Comparison of summer and winter inorganic carbon, oxygen and nutrient concentrations in Antarctic sea ice brine, *Mar Chem*, 51, 81–91, [https://doi.org/10.1016/0304-4203\(95\)00053-T](https://doi.org/10.1016/0304-4203(95)00053-T), 1995.
- Grotti, M., Soggia, F., Ianni, C., and Frache, R.: Trace metals distributions in coastal sea ice of Terra Nova Bay, Ross Sea, Antarctica, *Antarct Sci*, 17, 289–300, <https://doi.org/10.1017/S0954102005002695>, 2005.
- Günther, S. and Dieckmann, G. S.: Seasonal development of algal biomass in snow-covered fast ice and the underlying platelet layer in the Weddell Sea, Antarctica, *Antarct Sci*, 11, 305–315, <https://doi.org/10.1017/S0954102099000395>, 1999.
- Gutt, J., Starmans, A., and Dieckmann, G.: Impact of iceberg scouring on polar benthic habitats, *Mar Ecol Prog Ser*, 137, 311–316, <https://doi.org/10.3354/meps137311>, 1996.
- Hansen, H. P. and Koroleff, F.: Determination of nutrients, in: *Methods of seawater analysis*, edited by: Grasshoff, K., K. Kremling, and Ehrhardt, M., Wiley-VCH Verlag GmbH, 159–228, 1999.



- Hart, T. J.: Discovery Reports, Discovery Reports, VIII, 1–268, 1934.
- Hawco, N. J., Tagliabue, A., and Twining, B. S.: Manganese Limitation of Phytoplankton Physiology and Productivity in the  
720 Southern Ocean, *Global Biogeochem Cycles*, 36, e2022GB007382, <https://doi.org/10.1029/2022GB007382>, 2022.
- Hawkings, J. R., Skidmore, M. L., Wadham, J. L., Priscu, J. C., Morton, P. L., Hatton, J. E., Gardner, C. B., Kohler, T. J.,  
Stibal, M., Bagshaw, E. A., Steigmeyer, A., Barker, J., Dore, J. E., Lyons, W. B., Tranter, M., and Spencer, R. G. M.: Enhanced  
trace element mobilization by Earth’s ice sheets, *Proceedings of the National Academy of Sciences*, 117, 31648–31659,  
<https://doi.org/10.1073/pnas.2014378117>, 2020.
- 725 Helly, J. J., Kaufmann, R. S., Stephenson Jr., G. R., and Vernet, M.: Cooling, dilution and mixing of ocean water by free-  
drifting icebergs in the Weddell Sea, *Deep-Sea Research Part II-Topical Studies in Oceanography*, 58, 1346–1363,  
<https://doi.org/10.1016/j.dsr2.2010.11.010>, 2011.
- Henley, S. F., Cozzi, S., Fripiat, F., Lannuzel, D., Nomura, D., Thomas, D. N., Meiners, K. M., Vancoppenolle, M., Arrigo,  
K., Stefels, J., van Leeuwe, M., Moreau, S., Jones, E. M., Fransson, A., Chierici, M., and Delille, B.: Macronutrient  
730 biogeochemistry in Antarctic land-fast sea ice: Insights from a circumpolar data compilation, *Mar Chem*, 104324,  
<https://doi.org/10.1016/j.marchem.2023.104324>, 2023.
- Herraiz-Borreguero, L., Lannuzel, D., van der Merwe, P., Treverrow, A., and Pedro, J. B.: Large flux of iron from the Amery  
Ice Shelf marine ice to Prydz Bay, East Antarctica, *J Geophys Res Oceans*, 121, 6009–6020,  
<https://doi.org/10.1002/2016JC011687>, 2016.
- 735 Höfer, J., González, H., Laudien, J., Schmidt, G., Häussermann, V., and Richter, C.: All you can eat: the functional response  
of the cold-water coral *Desmophyllum dianthus* feeding on krill and copepods, *PeerJ*, 6, <https://doi.org/10.7717/peerj.5872>,  
2018.
- Höfer, J., Giesecke, R., Hopwood, M. J. M. J., Carrera, V., Alarcón, E., and González, H. E. H. E.: The role of water column  
stability and wind mixing in the production/export dynamics of two bays in the Western Antarctic Peninsula, *Prog Oceanogr*,  
740 174, 105–116, <https://doi.org/10.1016/j.pocean.2019.01.005>, 2019.
- Hopwood, M. J., Connelly, D. P., Arendt, K. E., Juul-Pedersen, T., Stinchcombe, M. C., Meire, L., Esposito, M., and Krishna,  
R.: Seasonal changes in Fe along a glaciated Greenlandic fjord, *Front Earth Sci (Lausanne)*, 4,  
<https://doi.org/10.3389/feart.2016.00015>, 2016.
- Hopwood, M. J., Cantoni, C., Clarke, J. S., Cozzi, S., and Achterberg, E. P.: The heterogeneous nature of Fe delivery from  
745 melting icebergs, *Geochem Perspect Lett*, 3, 200–209, <https://doi.org/10.7185/geochemlet.1723>, 2017.
- Hopwood, M. J., Carroll, D., Höfer, J., Achterberg, E. P., Meire, L., Le Moigne, F. A. C., Bach, L. T., Eich, C., Sutherland,  
D. A., and González, H. E.: Highly variable iron content modulates iceberg-ocean fertilisation and potential carbon export,  
*Nat Commun*, 10, 5261, <https://doi.org/10.1038/s41467-019-13231-0>, 2019.
- Huhn, O., Rhein, M., Kanzow, T., Schaffer, J., and Sültenfuß, J.: Submarine Meltwater From Nioghalvfjærdsbræ (79 North  
750 Glacier), Northeast Greenland, *J Geophys Res Oceans*, 126, e2021JC017224, <https://doi.org/10.1029/2021JC017224>, 2021.



- Joughin, I. and Vaughan, D. G.: Marine ice beneath the Filchner–Ronne Ice Shelf, Antarctica: a comparison of estimated thickness distributions, *Ann Glaciol*, 39, 511–517, <https://doi.org/10.3189/172756404781814717>, 2004.
- Kajanto, K., Straneo, F., and Nisancioglu, K.: Impact of icebergs on the seasonal submarine melt of Sermeq Kujalleq, *Cryosphere*, 17, 371–390, <https://doi.org/10.5194/tc-17-371-2023>, 2023.
- 755 Kim, K., Choi, W., Hoffmann, M. R., Yoon, H.-I., and Park, B.-K.: Photoreductive Dissolution of Iron Oxides Trapped in Ice and Its Environmental Implications, *Environ Sci Technol*, 44, 4142–4148, <https://doi.org/10.1021/es9037808>, 2010.
- Kim, S. and Collins, C. A.: Iceberg disturbance to benthic communities in McMurdo Sound, Antarctica, *Polar Record*, 57, e11, <https://doi.org/10.1017/S0032247421000048>, 2021.
- Kim, S., Saenz, B., Scanniello, J., Daly, K., and Ainley, D.: Local climatology of fast ice in McMurdo Sound, Antarctica, *Antarct Sci*, 30, 125–142, <https://doi.org/10.1017/S0954102017000578>, 2018.
- 760 Kim, S., Hammerstrom, K., and Dayton, P.: Epifaunal community response to iceberg-mediated environmental change in McMurdo Sound, Antarctica, *Mar Ecol Prog Ser*, 613, 1–14, <https://doi.org/10.3354/meps12899>, 2019.
- Kjær, H. A., Dallmayr, R., Gabrieli, J., Goto-Azuma, K., Hirabayashi, M., Svensson, A., and Vallenga, P.: Greenland ice cores constrain glacial atmospheric fluxes of phosphorus, *Journal of Geophysical Research: Atmospheres*, 120, 10, 810, 822, <https://doi.org/10.1002/2015JD023559>, 2015.
- 765 Knight, P. G., Patterson, C. J., Waller, R. I., Jones, A. P., and Robinson, Z. P.: Preservation of basal-ice sediment texture in ice-sheet moraines, *Quat Sci Rev*, 19, 1255–1258, [https://doi.org/10.1016/S0277-3791\(00\)00091-3](https://doi.org/10.1016/S0277-3791(00)00091-3), 2000.
- Krause, J., Hopwood, M. J., Höfer, J., Krisch, S., Achterberg, E. P., Alarcón, E., Carroll, D., González, H. E., Juul-Pedersen, T., Liu, T., Lodeiro, P., Meire, L., and Rosing, M. T.: Trace Element (Fe, Co, Ni and Cu) Dynamics Across the Salinity
- 770 Gradient in Arctic and Antarctic Glacier Fjords, *Front Earth Sci (Lausanne)*, 9, 878, <https://doi.org/10.3389/feart.2021.725279>, 2021.
- Krisch, S., Hopwood, M. J., Roig, S., Gerringa, L. J. A., Middag, R., Rutgers van der Loeff, M. M., Petrova, M. V., Lodeiro, P., Colombo, M., Cullen, J. T., Jackson, S. L., Heimbürger-Boavida, L.-E., and Achterberg, E. P.: Arctic – Atlantic Exchange of the Dissolved Micronutrients Iron, Manganese, Cobalt, Nickel, Copper and Zinc With a Focus on Fram Strait, *Global Biogeochem Cycles*, 36, e2021GB007191, <https://doi.org/10.1029/2021GB007191>, 2022.
- 775 Latour, P., Wuttig, K., van der Merwe, P., Strzepek, R. F., Gault-Ringold, M., Townsend, A. T., Holmes, T. M., Corkill, M., and Bowie, A. R.: Manganese biogeochemistry in the Southern Ocean, from Tasmania to Antarctica, *Limnol Oceanogr*, n/a, <https://doi.org/10.1002/lno.11772>, 2021.
- Laufer-Meiser, K., Michaud, A. B., Maisch, M., Byrne, J. M., Kappler, A., Patterson, M. O., Røy, H., and Jørgensen, B. B.: Potentially bioavailable iron produced through benthic cycling in glaciated Arctic fjords of Svalbard, *Nat Commun*, 12, 1349, <https://doi.org/10.1038/s41467-021-21558-w>, 2021.
- 780 Laufkötter, C., Stern, A. A., John, J. G., Stock, C. A., and Dunne, J. P.: Glacial Iron Sources Stimulate the Southern Ocean Carbon Cycle, *Geophys Res Lett*, 45, 13, 313–377, 385, <https://doi.org/10.1029/2018GL079797>, 2018.





- Lin, H. and Twining, B. S.: Chemical speciation of iron in Antarctic waters surrounding free-drifting icebergs, *Mar Chem*, 785 128, 81–91, <https://doi.org/10.1016/j.marchem.2011.10.005>, 2012.
- Lin, H., Rauschenberg, S., Hexel, C. R., Shaw, T. J., and Twining, B. S.: Free-drifting icebergs as sources of iron to the Weddell Sea, *Deep-Sea Research Part II-Topical Studies in Oceanography*, 58, 1392–1406, <https://doi.org/10.1016/j.dsr2.2010.11.020>, 2011.
- Loscher, B. M., DeBaar, H. J. W., DeJong, J. T. M., Veth, C., and Dehairs, F.: The distribution of Fe in the Antarctic Circumpolar Current, *Deep-Sea Research Part II-Topical Studies in Oceanography*, 44, 143–187, [https://doi.org/10.1016/S0967-0645\(96\)00101-4](https://doi.org/10.1016/S0967-0645(96)00101-4), 1997.
- Martin, J. H., Gordon, R. M., and Fitzwater, S. E.: Iron in Antarctic waters, *Nature*, 345, 156–158, <https://doi.org/10.1038/345156a0>, 1990.
- Meire, L., Meire, P., Struyf, E., Krawczyk, D. W., Arendt, K. E., Yde, J. C., Juul Pedersen, T., Hopwood, M. J., Rysgaard, S., 795 and Meysman, F. J. R.: High export of dissolved silica from the Greenland Ice Sheet, *Geophys Res Lett*, 43, <https://doi.org/10.1002/2016GL070191>, 2016.
- Meire, L., Mortensen, J., Meire, P., Juul-Pedersen, T., Sejr, M. K., Rysgaard, S., Nygaard, R., Huybrechts, P., and Meysman, F. J. R.: Marine-terminating glaciers sustain high productivity in Greenland fjords, *Glob Chang Biol*, 23, 5344–5357, <https://doi.org/10.1111/gcb.13801>, 2017.
- 800 Meredith, M. P., Inall, M. E., Brearley, J. A., Ehmen, T., Sheen, K., Munday, D., Cook, A., Retallick, K., Van Landeghem, K., Gerrish, L., Annett, A., Carvalho, F., Jones, R., Naveira Garabato, A. C., Bull, C. Y. S., Wallis, B. J., Hogg, A. E., and Scourse, J.: Internal tsunamigenesis and ocean mixing driven by glacier calving in Antarctica, *Sci Adv*, 8, eadd0720, <https://doi.org/10.1126/sciadv.add0720>, 2023.
- Moon, T., Sutherland, D. A., Carroll, D., Felikson, D., Kehrl, L., and Straneo, F.: Subsurface iceberg melt key to Greenland 805 fjord freshwater budget, *Nat Geosci*, <https://doi.org/10.1038/s41561-017-0018-z>, 2018.
- Mugford, R. I. and Dowdeswell, J. A.: Modeling iceberg-rafted sedimentation in high-latitude fjord environments, *J Geophys Res Earth Surf*, 115, <https://doi.org/10.1029/2009JF001564>, 2010.
- Nomura, D., Sahashi, R., Takahashi, K. D., Makabe, R., Ito, M., Tozawa, M., Wongpan, P., Matsuda, R., Sano, M., Yamamoto-Kawai, M., Nojiri, N., Tachibana, A., Kurosawa, N., Moteki, M., Tamura, T., Aoki, S., and Murase, H.: Biogeochemical 810 characteristics of brash sea ice and icebergs during summer and autumn in the Indian sector of the Southern Ocean, *Prog Oceanogr*, 214, 103023, <https://doi.org/10.1016/j.pocean.2023.103023>, 2023.
- Oerter, H., Kipfstuhl, J., Determann, J., Miller, H., Wagenbach, D., Minikin, A., and Graft, W.: Evidence for basal marine ice in the Filchner–Ronne ice shelf, *Nature*, 358, 399–401, <https://doi.org/10.1038/358399a0>, 1992.
- Oksanen, J., Blanchet, F. G., Friendly, M., Kindt, R., Legendre, P., McGlinn, D., Minchin, P. R., O’Hara, R. B., Simpson, G. 815 L., Solymos, P., H., M. H., Stevens, Szoecs, E., and Wagner, H.: *vegan: Community Ecology Package*, 2020.
- Parker, B. C., Heiskell, L. E., Thompson, W., and Zeller, E. J.: Non-biogenic fixed nitrogen in Antarctica and some ecological implications, *Nature*, 271, 651–652, <https://doi.org/10.1038/271651a0>, 1978.



- Peñuelas, J., Sardans, J., Rivas-ubach, A., and Janssens, I. A.: The human-induced imbalance between C, N and P in Earth's life system, *Glob Chang Biol*, 18, 3–6, <https://doi.org/10.1111/j.1365-2486.2011.02568.x>, 2012.
- 820 Person, R., Aumont, O., Madec, G., Vancoppenolle, M., Bopp, L., and Merino, N.: Sensitivity of ocean biogeochemistry to the iron supply from the Antarctic Ice Sheet explored with a biogeochemical model, *Biogeosciences*, 16, 3583–3603, <https://doi.org/10.5194/bg-16-3583-2019>, 2019.
- R Core Team: *R: A Language and Environment for Statistical Computing*, 2023.
- Raiswell, R.: Iceberg-hosted nanoparticulate Fe in the Southern Ocean: Mineralogy, origin, dissolution kinetics and source of bioavailable Fe, *Deep-Sea Research Part II-Topical Studies in Oceanography*, 58, 1364–1375, <https://doi.org/10.1016/j.dsr2.2010.11.011>, 2011.
- 825 Raiswell, R., Benning, L. G., Tranter, M., and Tulaczyk, S.: Bioavailable iron in the Southern Ocean: the significance of the iceberg conveyor belt, *Geochem Trans*, 9, <https://doi.org/10.1186/1467-4866-9-7>, 2008.
- Raiswell, R., Hawkings, J. R., Benning, L. G., Baker, A. R., Death, R., Albani, S., Mahowald, N., Krom, M. D., Poulton, S. W., Wadham, J., and Tranter, M.: Potentially bioavailable iron delivery by iceberg-hosted sediments and atmospheric dust to the polar oceans, *Biogeosciences*, 13, 3887–3900, <https://doi.org/10.5194/bg-13-3887-2016>, 2016.
- 830 Rapp, I., Schlosser, C., Rusiecka, D., Gledhill, M., and Achterberg, E. P.: Automated preconcentration of Fe, Zn, Cu, Ni, Cd, Pb, Co, and Mn in seawater with analysis using high-resolution sector field inductively-coupled plasma mass spectrometry, *Anal Chim Acta*, 976, 1–13, <https://doi.org/10.1016/j.aca.2017.05.008>, 2017.
- 835 Redfield, A. C.: On the proportions of organic derivations in sea water and their relation to the composition of plankton, in: *James Johnstone Memorial Volume*, edited by: Daniel, R. J., University Press of Liverpool, Liverpool, 177–192, 1934.
- Rignot, E., Jacobs, S., Mouginot, J., and Scheuchl, B.: Ice-Shelf Melting Around Antarctica, *Science* (1979), 341, 266–270, <https://doi.org/10.1126/science.1235798>, 2013.
- Robison, B. H., Vernet, M., and Smith, K. L.: Algal communities attached to free-drifting, Antarctic icebergs, *Deep Sea Research Part II: Topical Studies in Oceanography*, 58, 1451–1456, <https://doi.org/10.1016/j.dsr2.2010.11.024>, 2011.
- 840 Rozwalak, P., Podkowa, P., Buda, J., Niedzielski, P., Kawecki, S., Ambrosini, R., Azzoni, R. S., Baccolo, G., Ceballos, J. L., Cook, J., Di Mauro, B., Ficetola, G. F., Franzetti, A., Ignatiuk, D., Klimaszyk, P., Łokas, E., Ono, M., Parnikoza, I., Pietryka, M., Pittino, F., Poniecka, E., Porazinska, D. L., Richter, D., Schmidt, S. K., Sommers, P., Souza-Kasprzyk, J., Stibal, M., Szczuciński, W., Uetake, J., Wejnerowski, Ł., Yde, J. C., Takeuchi, N., and Zawierucha, K.: Cryoconite – From minerals and organic matter to bioengineered sediments on glacier's surfaces, *Science of The Total Environment*, 807, 150874, <https://doi.org/10.1016/j.scitotenv.2021.150874>, 2022.
- 845 Rudnick, R. L. and Gao, S.: Composition of the continental crust, in: *Treatise on geochemistry*, vol 3 *The Crust*, edited by: Holland, H. D. and Turekian, K. K., Elsevier, Amsterdam, 1–65, 2004.
- Schaffer, J., Kanzow, T., von Appen, W.-J., von Albedyll, L., Arndt, J. E., and Roberts, D. H.: Bathymetry constrains ocean heat supply to Greenland's largest glacier tongue, *Nat Geosci*, 13, 227–231, <https://doi.org/10.1038/s41561-019-0529-x>, 2020.
- 850



- Schwarz, J. N. and Schodlok, M. P.: Impact of drifting icebergs on surface phytoplankton biomass in the Southern Ocean: Ocean colour remote sensing and in situ iceberg tracking, *Deep Sea Res 1 Oceanogr Res Pap*, 56, 1727–1741, <https://doi.org/10.1016/j.dsr.2009.05.003>, 2009.
- 855 Sedwick, P. N., DiTullio, G. R., and Mackey, D. J.: Iron and manganese in the Ross Sea, Antarctica: Seasonal iron limitation in Antarctic shelf waters, *Journal of Geophysical Research-Oceans*, 105, 11321–11336, <https://doi.org/10.1029/2000jc000256>, 2000.
- Shaw, T. J., Raiswell, R., Hexel, C. R., Vu, H. P., Moore, W. S., Dudgeon, R., and Smith Jr., K. L.: Input, composition, and potential impact of terrigenous material from free-drifting icebergs in the Weddell Sea, *Deep-Sea Research Part II-Topical Studies in Oceanography*, 58, 1376–1383, <https://doi.org/10.1016/j.dsr2.2010.11.012>, 2011.
- 860 Smith Jr., K. L., Robison, B. H., Helly, J. J., Kaufmann, R. S., Ruhl, H. A., Shaw, T. J., Twining, B. S., and Vernet, M.: Free-drifting icebergs: Hot spots of chemical and biological enrichment in the Weddell Sea, *Science* (1979), 317, 478–482, <https://doi.org/10.1126/science.1142834>, 2007.
- Smith, J. A., Graham, A. G. C., Post, A. L., Hillenbrand, C.-D., Bart, P. J., and Powell, R. D.: The marine geological imprint of Antarctic ice shelves, *Nat Commun*, 10, 5635, <https://doi.org/10.1038/s41467-019-13496-5>, 2019.
- 865 Souchez, R., Meneghel, M., Tison, J.-L., Lorrain, R., Ronveaux, D., Baroni, C., Lozej, A., Tabacco, I., and Jouzel, J.: Ice composition evidence of marine ice transfer along the bottom of a small Antarctic Ice Shelf, *Geophys Res Lett*, 18, 849–852, <https://doi.org/10.1029/91GL01077>, 1991.
- Stephenson, G. R., Sprintall, J., Gille, S. T., Vernet, M., Helly, J. J., and Kaufmann, R. S.: Subsurface melting of a free-floating Antarctic iceberg, *Deep Sea Research Part II: Topical Studies in Oceanography*, 58, 1336–1345, <https://doi.org/10.1016/j.dsr2.2010.11.009>, 2011.
- 870 Stibal, M., Šabacká, M., and Žárský, J.: Biological processes on glacier and ice sheet surfaces, *Nat Geosci*, 5, 771–774, <https://doi.org/10.1038/ngeo1611>, 2012.
- Tranter, M., Skidmore, M., and Wadham, J.: Hydrological controls on microbial communities in subglacial environments, *Hydrol Process*, 19, 995–998, <https://doi.org/10.1002/hyp.5854>, 2005.
- 875 Trefault, N., De la Iglesia, R., Moreno-Pino, M., Lopes dos Santos, A., Gérikas Ribeiro, C., Parada-Pozo, G., Cristi, A., Marie, D., and Vaultot, D.: Annual phytoplankton dynamics in coastal waters from Fildes Bay, Western Antarctic Peninsula, *Sci Rep*, 11, 1368, <https://doi.org/10.1038/s41598-020-80568-8>, 2021.
- Vancoppenolle, M., Goosse, H., de Montety, A., Fichet, T., Tremblay, B., and Tison, J.-L.: Modeling brine and nutrient dynamics in Antarctic sea ice: The case of dissolved silica, *J Geophys Res Oceans*, 115, <https://doi.org/10.1029/2009JC005369>, 2010.
- 880 Vernet, M., Sines, K., Chakos, D., Cefarelli, A. O., and Ekern, L.: Impacts on phytoplankton dynamics by free-drifting icebergs in the NW Weddell Sea, *Deep Sea Research Part II: Topical Studies in Oceanography*, 58, 1422–1435, <https://doi.org/10.1016/j.dsr2.2010.11.022>, 2011.



- Wadham, J. L., Tranter, M., Skidmore, M., Hodson, A. J., Priscu, J., Lyons, W. B., Sharp, M., Wynn, P., and Jackson, M.:  
885 Biogeochemical weathering under ice: Size matters, *Global Biogeochem Cycles*, 24, <https://doi.org/10.1029/2009gb003688>,  
2010.
- Wehrmann, L. M., Formolo, M. J., Owens, J. D., Raiswell, R., Ferdelman, T. G., Riedinger, N., and Lyons, T. W.: Iron and  
manganese speciation and cycling in glacially influenced high-latitude fjord sediments (West Spitsbergen, Svalbard): Evidence  
for a benthic recycling-transport mechanism, <https://doi.org/10.1016/j.gca.2014.06.007>, 2013.
- 890 Wilson, N. J. and Straneo, F.: Water exchange between the continental shelf and the cavity beneath Nioghalvfjærdsbræ (79  
North Glacier), *Geophys Res Lett*, 42, 7648–7654, <https://doi.org/10.1002/2015GL064944>, 2015.
- Wu, S.-Y. and Hou, S.: Impact of icebergs on net primary productivity in the Southern Ocean, *Cryosphere*, 11, 707–722,  
<https://doi.org/10.5194/tc-11-707-2017>, 2017.
- Yang, Y., Ren, J., and Zhu, Z.: Distributions and Influencing Factors of Dissolved Manganese in Kongsfjorden and Ny-  
895 Ålesund, Svalbard, *ACS Earth Space Chem*, 6, 1259–1268, <https://doi.org/10.1021/acsearthspacechem.1c00388>, 2022.
- Yankovsky, A. E. and Yashayaev, I.: Surface buoyant plumes from melting icebergs in the Labrador Sea, *Deep Sea Research*  
Part I: Oceanographic Research Papers, 91, 1–9, <https://doi.org/10.1016/j.dsr.2014.05.014>, 2014.
- Zhang, R., John, S. G., Zhang, J., Ren, J., Wu, Y., Zhu, Z., Liu, S., Zhu, X., Marsay, C. M., and Wenger, F.: Transport and  
reaction of iron and iron stable isotopes in glacial meltwaters on Svalbard near Kongsfjorden: From rivers to estuary to ocean,  
900 *Earth Planet Sci Lett*, 424, 201–211, <https://doi.org/10.1016/j.epsl.2015.05.031>, 2015.